

CO_2 capture and recovery by the use of membrane crystallization

Dissertation presented by
Kevin SIMON

for obtaining the Master's degree in
Chemical and Materials Engineering

Supervisor(s)
Patricia LUIS ALCONERO, Israel RUIZ SALMON

Reader(s)
Jacques DEVAUX, Tom LEYSSENS

Academic year 2015-2016

Abstract

Nowadays CO_2 emissions are a global problem that requires immediate solutions. Membrane systems seem to be a promising solution due to their low energy consumption, their high mass exchange surface and their better scale-up possibilities. Moreover, conversion of CO_2 into Na_2CO_3 could lead to an interesting economic repurposing of the greenhouse gas.

That is why Na_2CO_3 recovery by using membrane distillation-crystallization was studied. In a very simple lab-scale system connecting a feed Na_2CO_3 solution and an osmotic $NaCl$ solution to one or two membrane modules, it was possible to produce $Na_2CO_3 \cdot 10H_2O$ crystals during more than one hour. Water removal is affected by both concentration and temperature, which can be adapted to control crystallization. Studies in larger scale systems have to be carried out to reinforce the promising results obtained in lab-scale system.

Acknowledgements

Before beginning this report, I would like to thank some people who contributed somehow to this present work.

First of all, I would like mainly to thank two persons who are for a lot in this work. On one hand my promoter, the Professor Patricia Luis, who trusted me and allowed me to collaborate with her. Her advice was very helpful to advance in this project. On the other hand, my supervisor, Israel Ruiz Salmon, for his availability, his help and his precious advice. I hope the results I have obtained will be helpful for the continuation of his PhD.

Other persons deserve acknowledgements for their help. Firstly, I would like to thank Luc Wautier and Frédéric Van Wonterghem who provided me with the chemicals and materials I needed to carry out my experiments. I am also thanking Ronny Santoro, who realised the chlorides titration for me. I am also very grateful towards Anne Vermaut, from the chemistry department, to have had the kindness to lend me a conductivity meter during several months while mine had a defect. I am appreciative to Raphaël Janssens, master thesis student last year on the same topic, whose the quality of the work helped me a lot to understand membrane techniques and to start my thesis. Moreover, although he was working on another personal project as PhD student, he spontaneously gave me some of his time to bring me advice, his opinions as well as teaching me to handle the experimental system.

I thank as well Professors Jacques Devaux and Tom Leyssens to have accepted to be my readers and assessors.

Finally, as this work consists in the end of my university course, I have a particular thought for all the professors I have attended the lessons these last six years. Their teaching allows to make me the future engineering graduate I am.

Contents

1	Introduction	13
2	Reviewing the State of the Art	14
2.1	Environmental state	14
2.1.1	Why are CO_2 emissions a problem?	14
2.1.2	Causes of the emissions	16
2.2	Current solutions for CO_2 capture	17
2.2.1	Pre-combustion capture	17
2.2.2	Oxy-fuel combustion capture	18
2.2.3	Post-combustion capture	19
2.3	Membrane techniques : generalities	21
2.4	Membrane contactors	23
2.5	Membrane distillation	27
2.5.1	Osmotic membrane distillation	27
2.5.2	Thermal membrane distillation	28
2.5.3	Mass transfer resistance	31
2.5.4	Heat transfer resistance	31
2.6	Membrane crystallization	32
2.6.1	Crystallization principles	32
2.6.2	Membrane crystallization	33
3	Objectives of the thesis	36
3.1	Overall objective of the research project: CO_2 capture by using membrane technology .	36
3.2	General and specific objectives of the Master thesis	37

4	Materials and methods	38
4.1	Chemicals and equipments used	38
4.1.1	Chemicals	38
4.1.2	Equipments	38
4.1.3	Preparation of the solutions	39
4.2	Experimental set-ups	41
4.2.1	First set-up: concentration influence	41
4.2.2	Second set-up: temperature influence	42
4.2.3	Third set-up: crystallization	43
4.2.4	Fourth set-up: two membranes in series	45
4.3	Experimental procedure	47
4.3.1	Flux characterization	47
4.3.2	Crystallization	47
4.4	Characterization and analyses	48
4.4.1	Conductivity meter	48
4.4.2	Flux measurement	48
4.4.3	Mass transfer coefficient	49
4.4.4	Average and standard derivations	49
4.4.5	Total water fraction	50
4.4.6	Quantitative analysis of Cl^- content by Charpentier-Volhard's method	50
4.4.7	Mass production estimation	52
5	Results and discussions	54
5.1	Influence of solutions concentration	54
5.1.1	Effects on the flux	54
5.1.2	Effects on mass transfer coefficient	55
5.2	Influence of temperature	57
5.2.1	Influence on the transmembrane flux	57
5.2.2	Influence on the mass transfer coefficient	58
5.3	Crystallization	58
5.3.1	Transmembrane flux	58
5.3.2	Duration before blocking	60
5.3.3	Total water fraction	62
5.3.4	Purity	62
5.3.5	Quantity produced	63
5.4	Influence of the variation of the surface area	63
5.4.1	Doubling the number of modules	63
5.4.2	One big or several smaller modules?	65
5.5	Practical example	66
6	Conclusion	69
	Bibliography	70
	Appendices	73
A	Activities calculation	73
B	Computation of required membrane surface	75
B.1	One unique module	75
B.2	Several modules in series	76

List of Symbols

Symbols	Signification	Units
A	Membrane area	m^2
a_f	Activity of the feed solution	-
a_p	Activity of the osmotic/permeate solution	-
C_0	Initial concentration	$\frac{g}{l}$
C_f	Final concentration	$\frac{g}{l}$
C_f	Concentration of the feed (Na_2CO_3)	$\frac{g}{l}$
C_o or C_p	Concentration of the osmotic/permeate solution	$\frac{g}{l}$
C_{new}	Concentration of the new solution	$\frac{g}{l}$
C_{old}	Concentration of the old solution	$\frac{g}{l}$
C_{sat}	Concentration at saturation	$\frac{g}{l}$
h_f	heat transfer coefficient between bulk feed solution and membrane	$\frac{W}{m^2 \cdot K}$
h_m	heat transfer coefficient through the membrane	$\frac{W}{m^2 \cdot K}$
h_p	heat transfer coefficient between bulk permeate/osmotic solution and membrane	$\frac{W}{m^2 \cdot K}$
I	Ionic strength	$\frac{mol_{solute}}{kg_{solvent}}$
J	Water transmembrane flux	$\frac{ml}{min \cdot m^2}$
J_{avg}	Average water flux through the membrane	$\frac{ml}{min \cdot m^2}$
J_{std}	Standard derivation of the transmembrane flux	$\frac{ml}{min \cdot m^2}$
K	Global mass transfer coefficient	$\frac{m}{Pa \cdot s}$
K_{avg}	Average mass transfer coefficient	$\frac{m}{Pa \cdot s}$
k_f	Mass transfer coefficient between bulk feed solution and membrane	$\frac{m}{Pa \cdot s}$
k_M	Mass transfer coefficient through the membrane	$\frac{m}{Pa \cdot s}$
k_p	Mass transfer coefficient between bulk permeate solution and membrane	$\frac{m}{Pa \cdot s}$
K_{std}	Standard derivation of mass transfer coefficient	$\frac{m}{Pa \cdot s}$
M_{AB}	Molality of the solution	$\frac{mol_{solute}}{kg_{solvent}}$
m_{added}	Added mass	g
$m_{crystals}$	Mass of crystals	g
m_f	Mass of the feed solution	g
m_i	Mass of the species i	g
M_m	Molar mass	$\frac{g}{mol}$ or $\frac{kg}{kmol}$
N	Transmembrane flux of the liquid	$\frac{ml}{min \cdot m^2}$
N	Number of experimental measurements	-
n_i	Number of moles of the species i	mol
P	Total pressure	Pa
p_f	Partial pressure in the feed solution	Pa

Symbols	Signification	Units
p_o	Partial pressure in the permeate/osmotic solution	Pa
p_{vap}	Vapor pressure	Pa
Q	Total heat flux	$\frac{W}{m^2}$
Q_0	initial flowrate	$\frac{ml}{min}$ or $\frac{l}{h}$
Q_f	final flowrate	$\frac{ml}{min}$ or $\frac{l}{h}$
Q_f	feed flowrate	$\frac{ml}{min}$ or $\frac{l}{h}$
Q_o	osmotic/permeate flowrate	$\frac{ml}{min}$ or $\frac{l}{h}$
$r_{p,max}$	Maximal pore size	m
T	Temperature	$^{\circ}C$ or K
t	Time	min
T_f	Temperature in the feed solution	$^{\circ}C$ or K
T_i	Temperature at the inlet	$^{\circ}C$
T_{lnmean}	Logarithm mean of the temperature	$^{\circ}C$
ΔT_m	Difference of temperature between both sides of the membrane	$^{\circ}C$ or K
T_o	Temperature at the outlet	$^{\circ}C$
T_p	Temperature in the permeate/osmotic solution	$^{\circ}C$ or K
TWF	Total water fraction of the crystals	%
U	Global heat transfer coefficient	$\frac{W}{m^2 \cdot K}$
V_f	Volume of the feed	l
V_{new}	Volume of the new solution	l
V_{old}	Volume of the old solution	l
$w_{anhydrous}$	Mass of pure Na_2CO_3 crystals + plate	g
w_{ini}	Mass of crystals formed during experiments + plate	g
w_{plate}	Mass of the plate	g
x_i	Liquid fraction of the species i	-
y_i	Vapor fraction of the species i	-
z^+ / z^-	Valence of the cation/anion	-
γ_{LV}	Surface tension between liquid and vapor phases	$\frac{N}{m}$
γ_{SL}	Surface tension between solid and vapor phases	$\frac{N}{m}$
γ_{SV}	Surface tension between solid and vapor phases	$\frac{N}{m}$
ΔP	Hydrostatic pressure	Pa
ΔP_{entry}	Breakthrough pressure or liquid entry pressure	Pa
Θ	Form factor of the pores	-
θ	Contact angle between solid-liquid and liquid-vapor interfaces	$^{\circ}$
λ	Molar heat of vaporization	$\frac{J}{mol}$
ν	number of ions present by molecules	-
ξ_i	Activity coefficient of the species i	-
ρ_{water}	Volumetric mass density	$\frac{g}{ml}$ or $\frac{kg}{m^3}$

Abbreviations	Signification
AGMD	Air gap membrane distillation
BPED	Bipolar electro dialysis
CCC	Carbon capture and conversion
CCS	Carbon capture and storage
DCMD	Direct contact membrane distillation
DEA	Diethanolamine

Abbreviations	Signification
GWP	Global warming potential
IPCC	International Panel on Climate Change
KSCN	Potassium thiocyanate
LEP	Liquid entry pressure
MA	Membrane absorption
MCr	Membrane crystallization
MDEA	Methyldiethanolamine
MEA	Methylethanolamine
NF	Nanofiltration
SGMD	Sweeping gas membrane distillation

List of Figures

2.1	CO_2 concentration evolution from about 400000 year ago to now.	15
2.2	Evolution of temperature and CO_2 emissions since 1850	15
2.3	Schema of the different CO_2 capture approaches.	18
2.4	Classical post-combustion absorption system, here applied for absorption with MEA.	20
2.5	Different kinds of membrane separation.	22
2.6	Principle of a pressure-driven membrane.	22
2.7	Contact angle θ between a liquid and a solid.	25
2.8	Polarization phenomenon in a $Na_2SO_4/NaCl$ system.	27
2.9	Condition of positive and negative flux in function of concentration in a $Na_2CO_3/NaCl$ system.	28
2.10	Comparison reverse osmosis and membrane distillation for concentratinf a orange juice.	29
2.11	Different kinds of membrane distillation.	30
2.12	Mass and heat transfer resistance model.	31
2.13	Classical phase diagram in function of the temperature and the concentration.	33
2.14	Picture of a fiber blocked by scaling.	35
2.15	Different ways to operate membrane crystallization	35
3.1	Flowsheet studied in the framework of Israel Ruiz Salmon's PhD.	36
4.1	Flowsheet of the first set-up.	41
4.2	Flowsheet of the second set-up.	42
4.3	Flowsheet of the third set-up.	43
4.4	Disposition of the tubes in the feed column.	44
4.5	Flowsheet of the fourth set-up.	45
4.6	Alternative flowsheet of the fourth set-up.	46
4.7	Calibration curves of the conductivity meter.	48
4.8	Phase diagram of Na_2CO_3	51
4.9	Simplified schema of the feed tank connected to the membrane.	52
5.1	Flux evolution during the experiment.	54
5.2	Flux evolution in function of the feed concentration	55
5.3	Flux evolution in function of time according that concentrations are left varying or not.	56
5.4	Mass transfer coefficient in function of the feed concentration	56

5.5	Transmembrane flux in function of the osmotic temperature for different feed temperatures.	57
5.6	Mass transfer coefficient in function of the osmotic temperature for different feed temperatures.	58
5.7	Average flux in function of the <i>NaCl</i> concentration when <i>Na₂CO₃</i> concentration is $215 \frac{g}{l}$	59
5.8	Mass transfer coefficient in function of the <i>NaCl</i> concentration when <i>Na₂CO₃</i> concentration is $215 \frac{g}{l}$	59
5.9	Operating duration before blocking appears in function of the osmotic concentration.	60
5.10	Picture of crystals during/after the experiment.	61
5.11	Mass, flux and concentration evolution during the experiment.	64
5.12	Transmembrane flux evolution according the number of modules used.	65
5.13	Schema of one module.	65
5.14	Schema of several modules in series.	66
A.1	Linear regression of the first Debye-Huckel coefficient.	73
B.1	Schema of one single module contactor.	75
B.2	Schema of several modules in series.	76

List of Tables

2.1	Growth rate of CO_2 concentration in air in the 6 last decades	15
2.2	List of the main greenhouse gases	16
2.3	Characteristics of pressure-driven membrane.	23
4.1	Technical informations about Liqui-Cel®2.5x8Extra-flow membrane.	39
4.2	Example of concentration variation during a typical experiment for different volume.	40
4.3	Classical methodology to prepare the solutions.	40
4.4	Experimental conditions used with the first set-up.	42
4.5	Experimental conditions used with the second set-up.	43
4.6	Experimental conditions used for the third set-up.	44
4.7	Experimental conditions used for the fourth set-up.	46
4.8	Total water fraction of Na_2CO_3 crystals.	50
5.1	TWF for different experimental conditions. Average and standard derivation.	62
5.2	Membrane area required for the crystallization step of a capture system for 330MW power plant, as well the quantity of crystals produced.	68
A.1	Debye-Huckel coefficients	74

Chapter 1

Introduction

Nowadays, pollution and the associated global warming are two of the biggest concerns in the world. By their industrial activities, humans release harmful compounds in atmosphere and water. Among the gases emitted, a category is responsible for the global warming Earth have to face. They are the greenhouse gases. Because of them, global Earth temperature has increased by 0.8°C since 1850 [1] and probably more since 1750s, period at which the Industrial revolution began.

The most regrettably known of these greenhouse gases is CO_2 . It is by far the most present and is single-handedly responsible for about two third of the total greenhouse effect [2]. Their atmospheric concentration increased by 43% since the birth of the industry around 1760 [3] and this tendency is just as topical as ever.

A possibility to motivate companies to invest in CO_2 struggle could be the production of a compound made from CO_2 that they could use or sell in order to make profits. It is in this kind of ideas that this master thesis places itself. Thanks to the efficiency of membrane techniques, CO_2 will be captured and converted in Na_2CO_3 , which can be used among others in ceramic industry [4].

This master thesis will mainly focus on the final step of the process, namely the Na_2CO_3 recovery by membrane crystallization. In this report, environmental state of the CO_2 emissions will be established as well the current solution to capture CO_2 . Afterwards, membranes technology will be introduced, particularly membrane distillation and membrane crystallization. Objectives of the thesis and experimental methods to fulfil them will be presented in the following. Finally, obtained results will be shown and consequences they involve will be explained.

Chapter 2

Reviewing the State of the Art

2.1 Environmental state

2.1.1 Why are CO_2 emissions a problem?

Greenhouse effect by atmospheric gases is a natural phenomenon, indispensable for the life on Earth. Indeed, it is responsible for global temperature on Earth and without it, temperature would be about $33\text{ }^\circ\text{C}$ lower [3]. Atmospheric gases absorb solar radiations reflected by Earth surface and send them back to the Earth, allowing to keep a part of their energy. By this way, temperature is not too hot and not too cold and ideal to allow to develop life.

So, why today do greenhouse gases have to be limited if they are good for Earth? Because, as many beneficial things, they lose their beneficial character when they are in excess. Since the beginning of the Industrial Revolution (about 1760), greenhouse gases concentration is still increasing and is responsible for the current global warming that Earth undergoes [2]. The main greenhouse gas is CO_2 , and studying its evolution with time perfectly illustrates the general tendency. As it can be seen on the Figure 2.1, CO_2 concentration fluctuated during ages, knowing periods of growth and decline. But it never exceeded a concentration of 300ppm. Today, humanity managed to go beyond 400ppm. The worst is this explosion of CO_2 concentration has occurred in only 250 years: in 1750, before the Industrial Revolution, CO_2 concentration in atmosphere was at 278ppm [3]. In 2014, it was at 397.7ppm, being an increase by 43% in comparison with the pre-industrial value [3]. The threshold of 400 ppm was passed in 2015 [1].

Temperature have the same kind of tendency. Figure 2.2a shows that between 1850s and 2000s, there is an increase of $0.8\text{ }^\circ\text{C}$ of the Earth global temperature, and Figure 2.2b clearly shows the correlation between CO_2 increase and temperature increase. Although it still remains some sceptics, this sad correlation is nowadays globally accepted. But a lot of efforts stay to be done as Table 2.1 proves it: CO_2 growth rate are still increasing whereas more and more people become aware of the problem and attempt to fight it.

In order to struggle against climate changes, CO_2 emissions have to be decreased. But it is not the only greenhouse gas existing. H_2O vapour is a natural greenhouse gas, as N_2O , CH_4 and also CO_2 [6]. They are basically present in atmosphere because they comes from natural phenomena in reasonable amount.

Unfortunately, human beings, by the way of industrial plants, widely increased the concentration of these gases. Even worse, their industrial activities introduced new greenhouse gases which have a

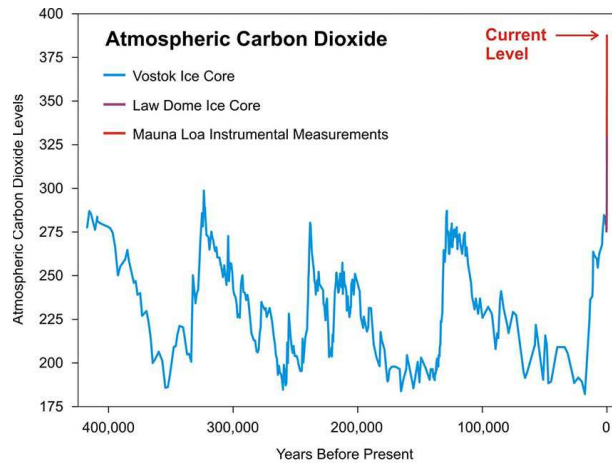
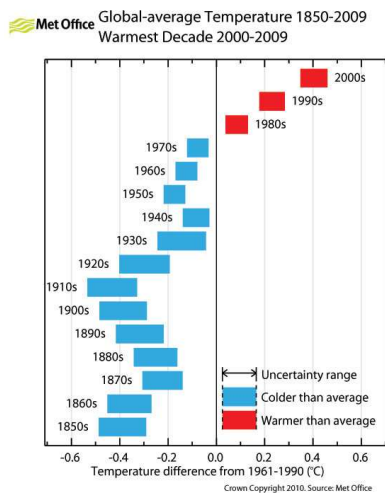
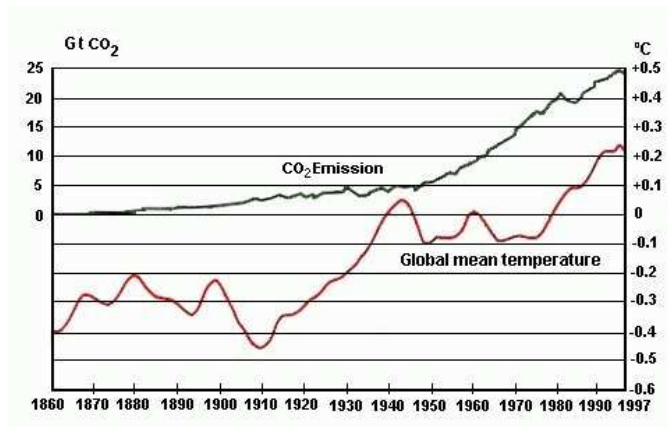


Figure 2.1: CO_2 concentration evolution from about 400000 years ago to now. Measurements have been done on ice caps in Antarctica. From [3].



(a)



(b)

Figure 2.2: Evolution of temperature and CO_2 emissions since 1850. From [1, 5]

Decade	Atmospheric CO_2 growth rate (in $\frac{ppm}{yr}$)
1959-1964	0.73
1965-1974	1.06
1975-1984	1.44
1985-1994	1.42
1995-2004	1.87
2005-2014	2.11

Table 2.1: Growth rate of CO_2 concentration in air in the six last decades. From [1].

much bigger global warming potential (GWP) than natural gases (Table 2.2). At same concentration, the GWP represents the capacity of a gas to keep the heat of the Earth [6]. The 25 value for CH_4 for instance means that the impact of a certain concentration of CH_4 on global warming is 25 times more important than the same concentration of CO_2 .

Even though other gases have a global warming potential much higher than CO_2 , their global effect is minor in comparison with the one of CO_2 . The reason is also visible on Table 2.2: their concentration in air is much lower than the CO_2 one. For most of them, their concentration does not reach ppb. That is why CO_2 is single-handedly responsible for two third of the global greenhouse effect [2], which explains the reason for which it is the major greenhouse gas against which solutions have to be found.

Gases	Concentration in 1750 (ppm)	Concentration in 2011 (ppm)	GWP	Atmospheric lifetime (yr)
Carbon dioxide (CO_2)	280	388.5	1	100
Methane (CH_4)	0.715	1.87/1.748	25	12
Nitrous oxide (N_2O)	0.27	0.323	298	114
CFC-12 (CCl_2F_2)	0	0.000533	10900	100
CF-113 (CCl_2CClF_2)	0	0.00000075	6130	85
HFC 23 (CHF_3)	0	0.000018	11700	270
HCFC-22 (CCl_2F_2)	0	0.000218	1810	12
HFC 134 (CF_3CH_2F)	0	0.000035	1300	14
HCFC-141b (CH_3CCl_2F)	0	0.00000022	725	9.3
HCFC-142b (CH_3CClF_2)	0	0.00000020	2310	17.9
HFC 152 (CH_3CHF_2)	0	0.0000039	140	1.4
Perfluoromethane (CF_4)	0.00004	0.00008	6500	50000
Perfluoroethane (C_2F_6)	0	0.000003	9200	10000
Sulfur hexafluoride (SF_6)	0	0.00000712	22800	3200

Table 2.2: List of the main greenhouse gases, their concentration in atmosphere and their potential impact on climate change. From [6]

2.1.2 Causes of the emissions

To better fight the increase of the emissions, it is important to know where they come from. Two kinds of emissions can be distinguished. On one hand, there are the natural emissions. They result from volcanoes eruptions, forest fires, ocean temperature oscillations [7] or more simply respiration of the living organisms. These emissions are not problematic.

On the other hand, there are the anthropogenic emissions. They are bound to human activities. Among them, 90% only comes from fossil fuels combustion, whose 38% in energy combustion plant [8]. That is why it is considered as the major contributor [9]. The rest is used as combustible in industries.

Industrial activities take part in 40% of the global emissions [10]. Some sectors stand out. Cement industry is responsible for between 20-26% of industrial emissions [10, 11], iron/steel industry takes part in 30% of the emissions and the chemical industry produces 17% of them [10]. Other contributions of human being to the emissions are also simply bounded to deforestation in their endless need of spaces and combustibles [10].

During eras, there were only the natural emissions which were counterbalanced by oceans and plants absorption. But for 200 years natural absorption have not been sufficient at all to compensate anthropogenic emissions [12]. Moreover, the still growing human population will increase the

products and energy demand [9, 10]. Renewable energy will not be able to fulfil the energy needs and unfortunately fossil fuels combustion will still remain the solution for many years [9]. That is why the question of CO_2 emissions has never been so crucial.

Governments became aware of these environmental problems and try to take measures to decrease the emissions. For example, International Panel on Climate Change (IPCC) has for goal to decrease by 50% the emission level from 1990 for 2050, which requires industries reduce their current emissions by 21% [9, 10]. European commission also develops documents presenting which are the current best available technologies (for example [5]) in order to reduce gases emissions. Applying them would allow to decrease the emissions by 12-23% [10]. But the assessment is the one of Table 2.1: the current emissions are far away of the expectations. That is why new technologies and solutions have to be found. The next section will present current approaches and solutions to CO_2 capture.

2.2 Current solutions for CO_2 capture

Currently, there are two global approaches to make the capture of CO_2 : carbon capture and storage (CCS) and carbon capture and conversion (CCC).

Carbon capture and storage (CCS): After the capture, CO_2 is compressed and concentrated to be stored permanently in the soil (oil/gas field, saline formations, immineable coal seals)[2, 10, 11]. It is currently one of the most promising solution in short term [13]. However, the big weak point of this approach is there is no guarantee about viability and safety in long term [10, 11, 13]. Underground redox conditions, microbial activity, risk evaluation associated to leakage are so many unknowns it remains to determine [11]. Moreover, this approach needs a lot of energy, especially for the compression before the storage and therefore it could be more polluting than eco-friendly [10, ?].

Carbon capture and conversion (CCC): The principle is to convert carbon in a stable and useful compounds [11]. The advantage of this approach is it tends towards being CO_2 neutral [2]. It is also less energy requiring than CCS and renewable energy can be used [11]. Nonetheless, the high stability of CO_2 related to its maximum oxidation state makes the energy demand for conversion non negligible [11]. Another advantage of CCC lies in the numerous fields of applications possible: improvement of alkaline solid waste, carbonated beverage, CO_2 -supplemented atmospheres in food production, supercritical CO_2 applications, medical, fire extinguisher, industrial pH control, asphyxiation of animals, biomass production, freezing, reagent in industry (a.o. ceramic industry), fuel production, polymer production, fertilizers, urea, methanol, esters, lactones, isocyanates, and so on. [2, 10, 11, 13, 14].

The post-capture objective (storage or conversion) will greatly depend on the choice of the absorption method. There are three main ways to carry out the CO_2 capture: pre-combustion capture, oxy-fuel combustion capture and post-combustion capture [6]. Figure 2.3 shows a representation of these three alternatives which will be explained in the next sections.

2.2.1 Pre-combustion capture

Pre-combustion capture (see Figure 2.3a) consists in a first time partially oxidising the fuel in a syngas (H_2/CO), then in a second step converting the CO in CO_2 thanks to a reaction with steam (water-gas shift)[10]. The oxidant in the first step can be O_2 (partial oxidation or gasification)(exothermic) or

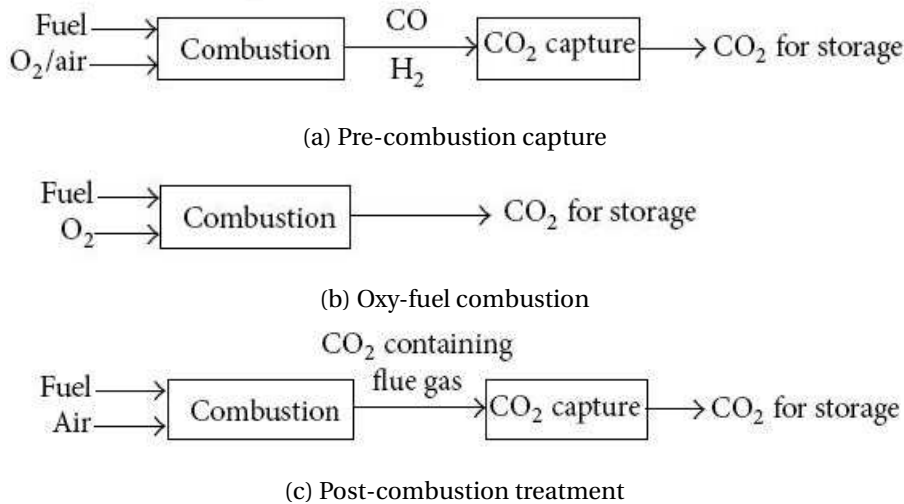


Figure 2.3: Schema of the different CO_2 capture approaches. From [6].

steam (steam reforming)(endothermic) [15]. Both can be combined in order that the heat produced by the partial oxidation serves to make the steam reforming [15].

The stream H_2/CO_2 resulting is separated by absorption [10]. The high pressure and concentration of the gas facilitate the absorption which can be easily done as well by a physical absorbent as by a chemical absorbent [10, 14]. The H_2 is then used as fuel in furnaces, engines, gas turbines or fuel cells [6]. The high pressure also allows to reduce the compression costs for storage [15].

Problem of this approach is the high energy and materials consumption, especially because the syngas needs to be cooled before the absorption [10]. Furthermore, technologies used in the process are expensive [6].

Pre-combustion capture can be used if the source of the emissions is the fuel but not when they comes from the reactants [10].

2.2.2 Oxy-fuel combustion capture

Oxy-fuel combustion (see Figure 2.3b) consists in a combustion of a pure oxygen stream (more than 95%) in order to have a highly concentrated combustion gases stream as product (mainly CO_2 and H_2O) [16, 17]. A part of the flue gas stream is recycled to dilute the oxygen stream because a too concentrated oxygen content will lead to a very hot flame [16]. The big advantage of this technique is the flue gas separation can be easily done by condensation at low cost while it is much more challenging in the other approaches [10].

If the flue gas separation is an advantage in comparison with the other techniques, O_2 separation from air (O_2/N_2 mixture) is the weak point of the oxy-fuel combustion since it requires cryogenic separation, which is highly expensive economically and energetically [16, 17].

Oxy-fuel combustion is used when the emissions source is the combustible but not when it comes from the raw materials [10].

2.2.3 Post-combustion capture

Post-combustion capture (see Figure 2.3c) consists in separating the CO_2 from the flue gas after a classical combustion step [14]. The big advantage of this approach with respect to the other ones is it does not need to adapt an existing plant. The absorption/stripping system is just put at the following of the process. Oxy-fuel combustions requires an air separation unit upstream and reactors needs to be slightly adapted to treat a much more concentrated oxygen stream. For pre-combustion capture, the combustible is H_2 so the reactor needs to be changed [6, 10]. Post-combustion approach also allows to capture CO_2 coming from raw materials, as it is the case in cement industry for example, which is clearly not the case of the two other approaches [10]. In consequence, post-combustion approach is widely the most used one [13].

Although post-combustion capture enjoys some non-negligible practical advantages, it also has some drawbacks. First of all, CO_2 in flue gas is not very concentrated: 12-15% mol due to the presence of N_2 and other combustion gases. Additionally, it is at atmospheric pressure. Thence the absorption is more difficult than in the other methods [10]. Moreover, CO_2 is in its more oxidised form and therefore quite few reactive [2]. Utilization of an absorbent with high affinity with CO_2 is for this reason needed [11]. Further, although they are lower than in pre-combustion, investment costs are not negligible at all, especially for big combustion plants. The absorber and stripper are responsible of 55% and 17% of the total cost, respectively [9]. Finally, pretreatment is required to remove impurities as SO_2 because they can interact with the absorbent [18].

As explained above, the choice of the absorbent is a critical point because of the low CO_2 content of the exhaust gas. Some post-combustion absorption system will be described in the following.

Absorption with amines

Absorption of CO_2 with amines is based on the chemical reaction between the alkaline amine group and the acid CO_2 [19]. Therefore they have a quite good reactivity and selectivity toward CO_2 despite the low CO_2 concentration [10, 12] making of them the best commercial sorbents at this level [11].

Absorption with aqueous amine solution is largely the most widespread technique due to its efficiency compared to the other post-combustion technique [11, 12]. Some used amine compounds can be listed, such as diethanolamine (DEA), methyldiethanolamine (MDEA) or piperazine [9]. But the reference technique and the most used is absorption with methylethanolamine (MEA) [10, 14, 20]. That is the reason a special look will be given to it.

Figure 2.4 shows a classical absorption with MEA system. In a first time, an absorption column will capture the CO_2 from flue gases. Then, in a second time, the CO_2 will be released and concentrated in the stripper, and the recovered absorbent is sent back to the absorber. MEA has a very good affinity and selectivity with CO_2 [10]. But it distinguishes itself from the other amines by a high kinetic reaction, allowing to capture more CO_2 despite short residence time [6]. Moreover, it can be easily synthesized from ammonia and ethylene oxide, two of the most produced compounds in the world [21]. Therefore, MEA is quite available and not too expensive.

Despite their efficiency and their wide use, alternatives to amines as absorbent are searched because of their inconveniences. Firstly, from an economic point of view, some losses of solvent can appear. Amines are very volatile compounds and losses can be the consequence of evaporation [12, 13]. For example, 1-4 ppm of MEA is found in the exhaust gases [11]. Some solvents are also lost by entrainment [20]. Moreover, they are not stable with respect to temperature [12] and impurities of the

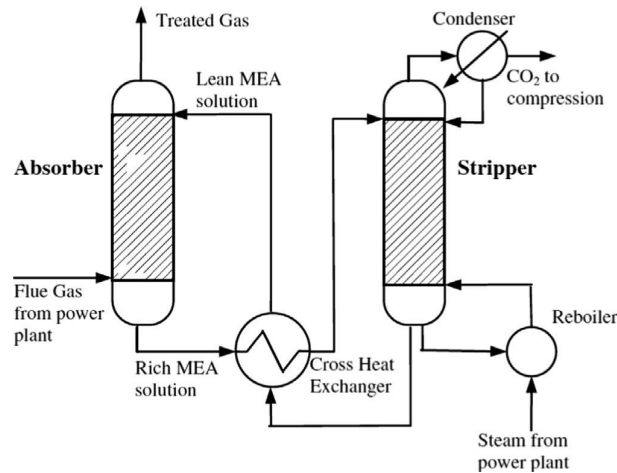


Figure 2.4: Classical post-combustion absorption system, here applied for absorption with MEA. From [9].

flue gas (SO_x , NO_x , H_2S , fly ash, heavy metals) [12]. For all these reasons, a make-up of amine solvent is required and rises at the order of $0.5\text{-}3.1\text{ kg}/\text{ton}_{CO_2}$ for MEA for instance [11, 20]. Furthermore, in the case of MEA, degradation can lead to very corrosive compounds which will attack and damage the equipments [9, 10, 11, 20, 21].

Another drawback of amine solvents, and probably the most problematic one due to their goal, is they are not really environmental friendly. First of all, amines are very toxic compounds, which is all the more prejudicial as they are volatile [11, 13]. Afterwards, amine solvents recovery needs a lot energy due to their high affinity with CO_2 [12]. For example, recovery of MEA requires $3.5\text{ GJ}/\text{ton}_{CO_2\text{ recovered}}$ [10]. The only fact of adding a post-combustion plant causes an increase of the electricity cost by 50-90% [10]. Nevertheless, on the plant scale, the CO_2 balance (CO_2 capture/ CO_2 emitted) is widely positive. But at a higher scale including ammonia and ethylene oxide production, the CO_2 balance is nearly negative. The reason is that ammonia synthesis is very energy consuming and produces a lot of CO_2 ($500\text{ kg}_{CO_2}/\text{tons}_{NH_3}$) [21]. Without a CO_2 capture system integrated in the ammonia production plant, the balance would be negative [11].

Calcium looping

Calcium looping technology uses CaO as adsorbent. In a first step, CO_2 is captured according a carbonation reaction:



In a second step, the adsorbent is recovered by a calcination reaction, which is simply the reverse of Equation 2.1. As a result, CO_2 is released for storage [22]. The CaO regenerated is sent back in the carbonator for a new cycle. Both reactions have very good kinetics, which allows to operate with low residence time [11].

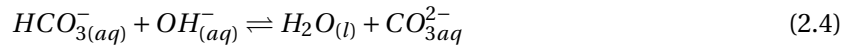
Advantage of this solution is the cheapness of the adsorbent, which is very available [11]. It could be interesting to couple a cement industry, a power plant and a calcium looping capture system. By the way, 94% of the emissions could be avoided by this coupling [11]. However, the CaO is quickly saturated and efficiency decreases with the number of cycles [11]. Moreover, some impurities, especially SO_2 , forms relatively stable compounds ($CaSO_4$) with CaO , leading to adsorbent elimination [18].

This technique can be used for CO_2 storage, but could also be used for valuable compounds production [11].

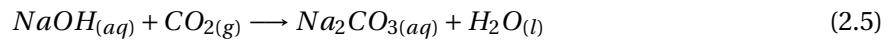
Alkaline solutions ($NaOH$)

Strong alkaline solutions can be also used as absorbent and take advantage of the acid character of CO_2 . Among them, a particular attention will be devoted to $NaOH$ absorption.

The absorption mechanism is based of a CO_2 dissolution then a reaction with hydroxide ions coming from $NaOH$ presence (entirely dissociated in Na^+ and OH^-) according to the following model [20]:



The global reaction is, taking into account the $NaOH$ dissolution:



Advantages to use $NaOH$ compared with MEA is a better absorption capacity and it is cheaper too [18, 20]. However, MEA has a higher capture rate. But this disadvantage can be corrected by increasing $NaOH$ concentration.

Generally, absorption with $NaOH$ is not used for soil storage due to the difficulties to recover the solvent. The reason is firstly the high solubility of the formed product ($NaHCO_3$) and secondly, the crystals formed (Na_2CO_3) are very stable and require a temperature above $800^\circ C$ to decompose themselves and release CO_2 [9, 20]. That is why absorption with $NaOH$ is rather used to produce Na_2CO_3 crystals, which could be used in industry.

2.3 Membrane techniques : generalities

The previous section presented different solutions for CO_2 already applied or under research. Another potential solution not presented above and deserving a special attention are the ones based on membrane technologies. Research showed they present advantages which make them a promising alternative for CO_2 capture in the future, especially compared with the absorption columns present in each one of the aforementioned processes.

A membrane is a porous barrier aiming to separate different phases (gas and liquid). Membrane technology can be divided in two general approaches according to how the separation occurs due to the selectivity or not offered by the membrane. [10]. These different techniques are illustrated at the Figure 2.5.

The first way to perform the separation is thanks to selective membranes. The principle is based on a better diffusion of one of the species in comparison with the other ones because the membrane selectivity towards one of the compounds. Therefore, a bigger quantity of the wanted compound will be in one side and the other compounds in the other side [2, 11]. Selective membranes can be split

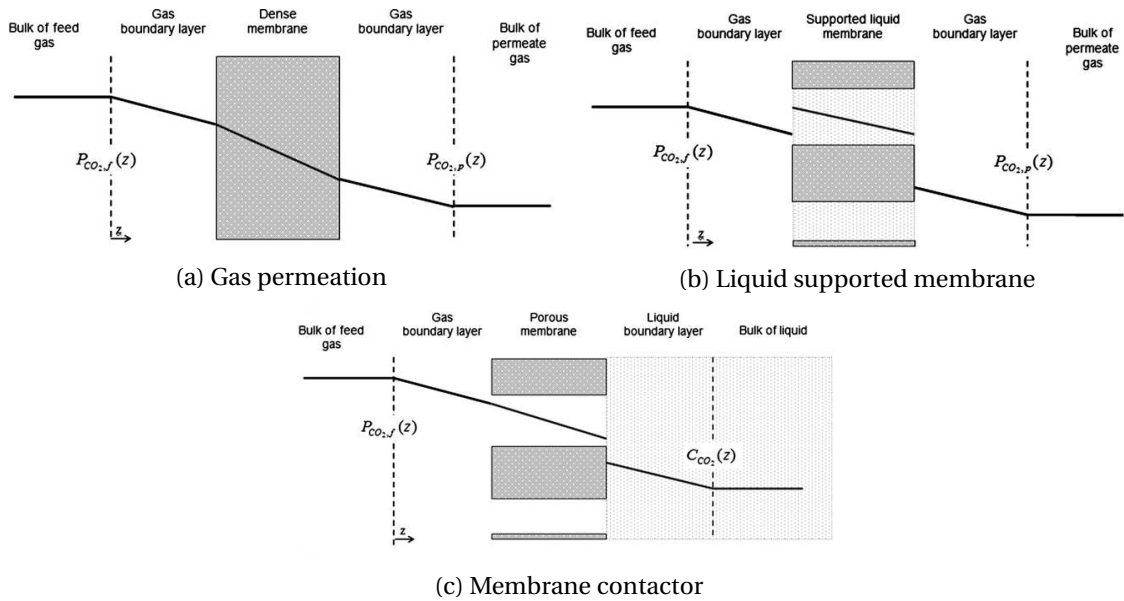


Figure 2.5: Different kinds of membrane separation. From [10]

in two different manners to operate. The first way is gas permeation (see Figure 2.5a) where it is a dense membrane which limits the diffusivity and solubility of the compounds by the material which constitutes it. This technique is limited to gas phase. In the framework of CO_2 capture, it only has potential for pre-combustion capture [10, 11]. Secondly there is supported liquid membrane (see Figure 2.5b). Here, the pores are filled with a liquid (for instance ionic liquid [10]) which will carry out the diffusion selectivity. Its field of applications in CO_2 capture is broader than gas permeation as it can be used for pre- and post-combustion capture [10, 11].

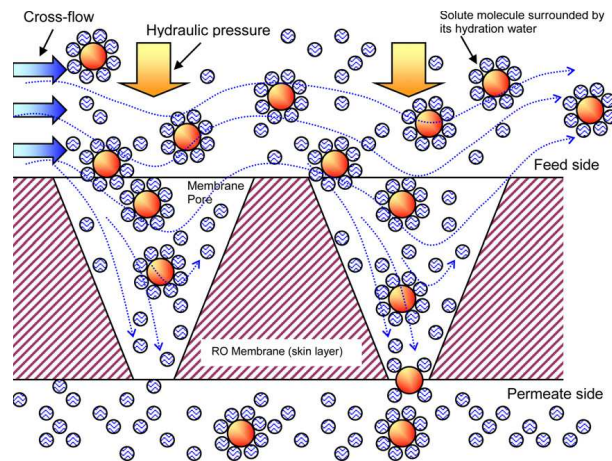


Figure 2.6: Principle of a pressure-driven membrane. From [23].

Another separation techniques using membrane is pressure-driven membrane. Under the effect of pressure, a liquid solution is forced to cross a membrane. The solid particles are simply retained by the pores of the membrane according to the size particles, their charge or their affinity with the membrane (see Figure 2.6) [24, 23, 25]. Micro-filtration, ultra-filtration, nano-filtration and reverse osmosis can be classed in this category [26]. These processes are different on their pore size and therefore the pressure applied, as Figure 2.3 shows it. They can be used for purification [26], separation [26], concentration

[24] or crystallization [27] in different fields of applications: seawater desalination, waste treatment, food industry, biomedical, bioseparation [26, 28]. The drawbacks of these techniques are a high energy consumption bounded to the high pressure used (especially for nanofiltration and reverse osmosis) and a poor resistance against fouling [26].

	Microfiltration	Ultrafiltration	Nanofiltration	Reverse Osmosis
Pore size (μm)	$10^{-1} - 10$	$10^{-3} - 10^{-2}$	10^{-3}	10^{-4}
Pressure (bar)	0.2-1	1-5	3-15	10-100

Table 2.3: Characteristics of pressure-driven membrane. From [24, 25]

2.4 Membrane contactors

The other way to make the mass transfer is via a non dispersive contact by means of micro-porous membrane or membrane contactor (see Figure 2.5c). The membrane just separates physically the two phases. It does not have a selective role [10, 11, 29]. Contacts between phases are due to the pores [10]. The exchange is done because of a driving force generated by a chemical potential reduction and forces some compounds to cross the membrane. Compared with selective membranes, non dispersive membranes enable better transfer between phase because pores are filled with gas and diffusion is easier in gas phase [10] and offers less resistance than for example dense membrane because of wider pores [19]. It can be used for gas-liquid system as represented on Figure 2.5 but also for liquid-liquid system [2]. Consequently, applications with this kind of membrane are numerous and can substitute plenty of classical separation methods. Membrane contactors can be used for absorption and stripping [13], distillation [7, 29], gasification [10], crystallization [14, 18, 29, 30, 31, 32, 33], liquid-liquid extraction [29] and even chemical reactions [29]. Applied for CO_2 capture, this kind of membranes are essentially used for post-combustion capture [10].

If membranes are seen as alternatives to plenty of current technologies such as absorption and distillation columns and as a possibility for CO_2 capture, it is for the sake of its numerous advantages.

Firstly, membranes are mainly characterized by their surface area, which is fixed and accurately known [19, 29]. In absorption and distillation tower, contact surface between gas and liquid is dependent on the flowrate of each phase [2].

Secondly, membrane contactors allows to seriously reduce equipments size due to their compactness [29]. Their specific area will depend on their configuration (flat membrane, tubular, spiral wound, hollow fibers) [29]. But the most compact one is a hollow fibers disposition which allows specific areas comprised between 1500 and 6500 m^2/m^3 [19, 29]. In comparison, classical towers are specific areas between 30 and 800 m^2/m^3 [19, 29]. It can be easily explained by the size of the constitutive elements of each devices. Hollow fibers are very little cylindrical tubes of less than 1 mm diameter. For example, liqui-cel®2.5x8 extra-flow membrane contactors¹ has fibers of 300 μm diameters [34]. In absorption or distillation tower, packing or holes of trays are several cm size [24]. For a same volume, membrane contactors offer a higher interfacial area, which enables better exchanges and higher mass and heat transfer [19, 29, 35].

Other advantages of membrane contactor are bounded to separation role of membranes. First of all, the two different phases are not mixed. In consequence, there is no need to separate them in post

¹It is the one used for the experiments (see Section 4.1.2).

treatment operation [29]. It also allows to work with fluids of different densities [29]. Furthermore, it enables to avoid often encountered problems in absorption and distillation columns: flooding, foaming, entrainment or weeping [13][29]. These phenomena occur when gas and liquid flow rates are too high or too low and because the phases are in contact [24]. Consequently, a certain flexibility is possible for the operating flow rate in membrane contrary to classical methods [29]. More generally, membranes offer more flexibility in operating conditions and configurations in function of the treatment needs than their classical counterparts [9, 11, 29].

In addition to the previous advantages, membranes allow better fluid distribution than the classical methods [35]. It is logical because tubes are small and homogeneity is easier to obtain than in several meters diameter columns or tanks. Moreover, a very selective mass transfer can be achieved by using the right operating conditions [35].

Finally, there are two big non negligible advantages of membrane techniques. On one hand, they are much less energy consuming than their classical counterparts [10, 11, 13]. It can be explained by an higher exchange area and therefore an efficient mass transfer that the classical method can only reach by increasing temperature, pressure, and so on. Additionally, membranes offer low pressure drop so less pumping costs [29]. By the way, this low energy consumption motivates their use for CO_2 capture. On the other hand, the simplicity of membrane techniques greatly facilitates the scale-up: adding membrane modules increases the capacity linearly [9, 29, 35].

If membranes have numerous advantages, there are still some challenges to improve them. Paradoxically, although membrane allows to increase the mass transfer, it is also a natural barrier offering an extra resistance to this one [11, 35]. Thanks to their higher interfacial area, membranes compensate this resistance and enable higher mass transfer than the classical method [19]. But because of this, mass transfer coefficient is the same, even slightly lower, as the classical methods [29]. An appropriate use of the membranes can greatly limit this extra resistance.

Another problem of membranes is they are subject to degradations and technical issues which, if few attentions are paid on them, membranes life time and their efficiency will be greatly reduced [29]. It is problematic because membrane are quite expensive and as a result, it greatly threatens their economical viability compared with classical method [13, 29]. An example of degradation is, in the framework of membrane absorption, the use of some solvents which could degrade the membrane [2][13]. Other phenomena such as wetting, fouling and scaling lead to equivalent results [29]. Origins, physical principles behind the three latter ones as well as solutions to limit them are described in the sections below.

Wetting

In membrane contactors, pores are normally filled with gas. But after a certain time, liquid can enter the pores. The liquid-gas interface is not outside the pore anymore but inside of it. This phenomenon is called wetting. The reason for which it is problematic is that it creates a extra mass transfer resistance [10, 14, 19].

The wetting is mainly due to the affinity between the liquid and the membrane material. If there is a good affinity between them, liquid droplets will have a tendency to form in the pore. The phenomena can be explained by the Figure 2.7 and the Young equation [29] :

$$\gamma_{LV} \cos(\theta) = \gamma_{SV} - \gamma_{SL} \quad (2.6)$$

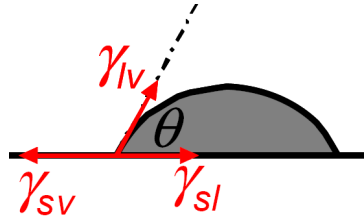


Figure 2.7: Contact angle θ between a liquid and a solid. γ_{sv} , γ_{lv} and γ_{sl} are the surface tension between solid and vapor, liquid and vapor, solid and liquid respectively.

θ is the contact angle. γ is the surface tension between liquid and vapor phase (LV), solid-vapor (SV), solid-liquid (SL). The more the liquid will have a strong affinity with the solid membrane, lower the surface tension between them will be and then the contact angle too, which will favour droplets formation and wetting. That is why, in order to prevent from wetting, membrane and liquid must have low affinity. When liquid is hydrophobic, membrane has to be hydrophilic, and when liquid is hydrophilic (as aqueous solution), the membrane has to be hydrophobic (such as polypropylene for example) [13, 29]. Furthermore, liquid affinity with the membrane can be affected by other compounds the solution contains such as amines (for example in absorption), impurities, detergents, surfactants, other solvents [19, 29].

The tension surface and affinity between the liquid and the solid are just a resistance against wetting. If you use the most hydrophilic solvent with the most hydrophobic membrane, wetting can occur if hydrostatic pressure is too high. This fact can be explained by the existence of a breakthrough pressure or liquid entry pressure (LEP) described by the Laplace equation [29]:

$$\Delta P_{entry} = -\frac{2\Theta\gamma\cos(\theta)}{r_{p,max}} \quad (2.7)$$

where $r_{p,max}$ is the maximum pore size, γ is the interfacial tension and Θ a geometric factor related to the form of the pores. For cylindrical pore, $\Theta = 1$. If the operating pressure is above the breakthrough pressure, wetting will occur [7, 19, 29]. Therefore, higher the liquid entry pressure will be, the more the wetting will be prevented. It will be the case through the contact angle factor if a membrane having a poor affinity with the liquid is used as aforementioned. Similarly, a membrane with very small pores will prevent from wetting [7, 13, 29]. However, if the liquid pressure has to be lower than the liquid entry pressure, it also has to be slightly higher than the pressure of the vapour phase (if there is one) to avoid gas bubbles apparition and dispersion in the liquid [19, 29]. Another reason of wetting can be capillary condensation on the pore walls of the vapor phase [19].

Wetting is a phenomenon which will occur if sufficient long time is left to the system. However, the time after which the wetting appears can be greatly delayed by watching out for operating conditions [13, 35]. Moreover, once wetting appeared, decreasing the pressure to restore un-wetted condition will not work given that the liquid transfer will, from this point forward, follow the linear Darcy law ($N = K \cdot \Delta P$) [29]. System have to be stopped to remove wetting.

Scaling and fouling

Scaling and fouling problems are due to the deposit of solid matter on the membrane surface, leading to a pore blockage and a decrease of the mass transfer [35]. These phenomena will occur after a certain time of operation [35] which could be more or less long according to the operating condition

and the care brought to delay it.

Difference between scaling and fouling are just related to the origin of the deposits. Scaling (or inert-fouling) results from inorganic matters deposition. It could be due to solid materials formation in the framework of membrane crystallization or precipitation and accumulation of impurities with operating time [7]. To the contrary, fouling (or bio-fouling) has an organic origin. It results from the deposition of dissolved organic matters or the development of micro-organisms [2, 7].

Both phenomena will depend on flows characteristics, membrane material and operating conditions (example: temperature since solubility of most of compounds is temperature dependant) [7]. Usually, membranes made in polymer have good resistance against fouling [35].

Scaling can be delayed by increasing the diameter of the tubes [35]. Anti-scalant additives can be also used but as a lot of them are organic compounds, it will decrease the hydrophilic character of an aqueous solution for example and favour wetting [7, 35]. Otherwise, rinsing and cleaning the membrane will remove the deposited particles regardless of their origin [7].

Polarization

Polarization is the concentration or temperature gradient that appears between the bulk fluid and the membrane [29, 36]. In the case of a difference of concentration, it is called "concentration polarization" and in the case of temperature "temperature polarization". Polarization phenomenon is a consequence of the removal (or addition, in function of the membrane side) of the compounds. Removing water from the solution for instance will increase concentration of a compound near the membrane and this one will be higher than the one in the bulk. Polarization has a negative impact on the mass or heat transfer because it decreases the concentration/temperature difference between both sides of the membrane [36].

Polarization is a phenomenon related to fluid dynamics. The only way to reduce it is to generate mixing and turbulence in the flow to decrease the thickness of the boundary layer. One way to do that is simply increasing the flow rate (see Figure 2.8) [14, 31]. But there is also a maximum value of the flow rate above which it is useless to rise because the mixing is sufficient enough to ensure good homogeneity. Incidentally, it is better not to go up above this flow rate to prevent wetting. Another way to increase turbulence is to use spacers, which will force flow to skirt them and by this way generate Eddy currents [29]. Finally, polarization can appear in each side of the membrane. Therefore, both flow rates have to be maximised [31].

Finally, there are few informations about membrane behaviours at industrial scale, especially in field of the resistance against the aforementioned degradations and their long term efficiency [11, 35]. Companies seem unfortunately but logically few inclined to try membrane technologies in place of the technologies they are using for many years and give satisfying results.

To sum up, a good membrane must be responsible for a high mass transfer, have a high packing density to increase the available surface, present a low pressure drop, prevent wetting and scaling, and of course be non-reactive with the fluids in presence [7].

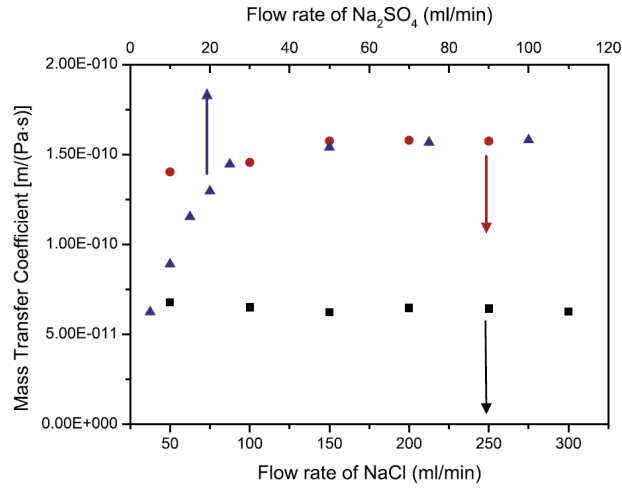


Figure 2.8: Polarization phenomenon in a $Na_2SO_4/NaCl$ system. It can be seen that if the Na_2SO_4 flow rate (triangle) is increased, mass transfer coefficient increases too. From [31]

2.5 Membrane distillation

Membrane distillation consists in a system with one liquid in the retentate side and a fluid (liquid or gas) in the permeate side. A component of the retentate (generally the solvent) will cross the membrane after evaporation and condensate in the permeate side [7, 29]. This technique is used to concentrate the retentate or purify it [29].

The evaporation of the solvent is motivated by a solvent partial pressure gradient [29]. The solvent transmembrane flux J is given by [37]:

$$J = K(p_f - p_o) \text{ with } p_i = P \cdot y_i = p_{vap}^0 \cdot a_i = p_{vap}^0 \cdot \xi_i \cdot x_i \quad (2.8)$$

In this expression, K is the global mass transfer coefficient ($\frac{m}{Pa \cdot s}$), p_i is solvent partial pressure (Pa) of the corresponding side (f for feed, o for osmotic), P stands for the total pressure, p_{vap}^0 is the vapor pressure, x_i is the liquid fraction, y_i the gas fraction, a_i is the activity and ξ_i is the activity coefficient. There are two ways to generate the solvent partial pressure gradient: by a concentration gradient (osmotic membrane distillation) or by a temperature gradient (thermal membrane distillation). Both gradients can be associated synergetically or antagonistically [29].

Using osmotic membrane distillation or thermal membrane distillation carries some advantages compared to use classical distillation. Firstly, the gain in space due to the compactness of the membrane [7]. Secondly, it can be used with all membrane dispositions (flat sheet, spiral, tubular, hollow fibers, ...). Finally the used temperature is much lower in membrane distillation than in column distillation. It allows to use it for labile or poorly temperature resistant compounds [2]. Moreover, low-grade energy as solar energy, or waste heat from the system can be used to warm the retentate [7, 29, 38].

2.5.1 Osmotic membrane distillation

Osmotic membrane distillation generates a partial vapour gradient by the way of a difference of activities between the retentate or feed side and the permeate or osmotic side. Generally, it is mainly due to a concentration gradient between both sides, but nature of the species are important

too through the ionic strength of the solution. The goal is to remove the solvent to concentrate the feed solution or to remove another compound to purify the feed. To that purpose, the osmotic solution will be an hypertonic solution, with a very high concentration of salt and a lower concentration of solvent than in the feed solution [29].

As the evaporation is generated by a concentration gradient, a lower feed concentration and a higher osmotic concentration will occasion a higher mass transfer [14, 31]. Notice that it is possible to have a negative flux by having a too high feed concentration and too low osmotic one: the water will evaporate from the osmotic side to condensate in the feed one, what is not desired (see Figure 2.9)[14]. The nature of the ions will also be important. For example, at same mass concentration, a $MgCl_2$ osmotic solution will generate an higher transmembrane flux than a $NaCl$ one [14]. The reason is that $MgCl_2$ generates 3 ions (1 Mg^{2+} and 2 Cl^-) and $NaCl$ only two (1 Na^+ and 1 Cl^-). The ionic strength is therefore higher for $MgCl_2$ than for $NaCl$ (see Appendix A).

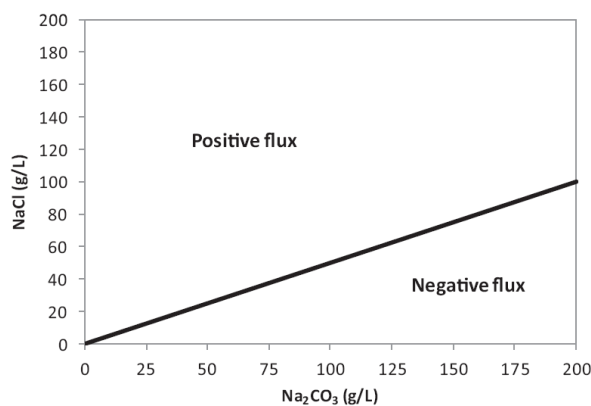


Figure 2.9: Condition of positive and negative flux in function of concentration in a $Na_2CO_3/NaCl$ system. $NaCl$ concentration has to be superior to the half of Na_2CO_3 concentration to obtain non-negative flux. From [14]

Although basically this distillation operates in isothermal condition (no temperature gradient between both sides), a slight local temperature gradient can appear in each side between the bulk and the membrane. The reason is that solvent evaporates to migrate toward the permeate, which requires to take energy of the system. Solvent condensation releases energy. Ergo it heats the osmotic solution [29].

Advantage of osmotic distillation comparing with thermal distillation is the possibility to work with labile or not thermally resistant compounds [29]. Moreover, it consumes less energy as there is no need to heat and cool. Osmotic membrane distillation is classically use for removal of volatile compounds such as alcohol from water for example [29], concentration of pharmaceutical compounds [32] or carbonate and sulphate compounds [14, 31].

2.5.2 Thermal membrane distillation

Thermal membrane distillation (or more simply membrane distillation) consists in separating a hot retentate solution from a cold permeate one. By this way, the difference of vapor pressure is due to a temperature gradient [7, 29, 38]. The higher the temperature difference between both sides is, the higher the mass transfer is [2].

Membrane distillation due to temperature gradient have some advantages to be used in comparison with this column counterpart. Firstly, even though it requires heating, cooling and energy, the energy demand is much lower than a classical distillation column, because the operating temperature is lower. Incidentally, the temperature in membrane distillation is low (generally 30–60°C [37] although there are some rare applications at 130°C [39, 40]) so that it is possible to heat and cold the flow by using low grade energy, such as solar or geothermal energy [7, 29, 38], and even waste heat of the system [2].

Membrane distillation has some advantages justifying to choose it in place of other techniques. First of all, it is possible with very concentrated feed [7]. Moreover, compared with reverse osmosis which is the other very used membrane concentration technique, it is more efficient to use membrane distillation for high feed concentration than using reverse osmosis. It is not the case at low concentration (see Figure 2.10) [29, 37]. The reason is that the higher feed concentration is, the higher the ionic strength and so osmotic pressure is. Reverse osmosis needs very high pressures to continue to ensure a correct flux whereas thermal membrane distillation is quite few affected by the phenomena since most of its driving force comes from temperature gradient [37]. Further, feed pretreatment is less necessary than in reverse osmosis because membrane distillation is less sensitive to feed variation. The hydrostatic pressure is lower too [7]. Compared to distillation column, in addition to the compactness, membrane distillation also allows to separate azeotropic mixture, which is very difficult in classical distillation [29]. Finally high solute rejection can be achieved [7].

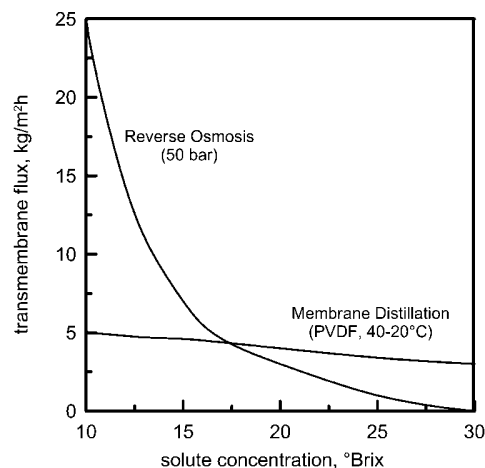


Figure 2.10: Comparison reverse osmosis and membrane distillation for concentration of an orange juice. From [37].

Nevertheless, membrane distillation has some disadvantages. First of all, there is no available material designed specifically for membrane distillation [29]. It causes a lot of energy losses by conduction [29]. Therefore, heat transfer is often inefficient and it leads to low permeate flux [7]. Heat losses could be limited by using an optimal module geometry and by using a membrane material with a low thermal conductivity [29]. Moreover, compared to reverse osmosis and osmotic distillation, there is a higher energy consumption due to heating and cooling [7, 29]. But contrary to reverse osmosis, it requires low pressure cost, which balances the high heating/cooling energy in total energy consumption.

Membrane distillation is mainly used to produce ultra pure water or to concentrate aqueous solution [29] and in desalination [39, 40].

Kind of membrane distillation

There are 4 different ways to operate in membrane distillation: direct contact, air gap, sweeping gas and vacuum membrane distillation (see Figure 2.11). All of them are related what the distillate side consists in.

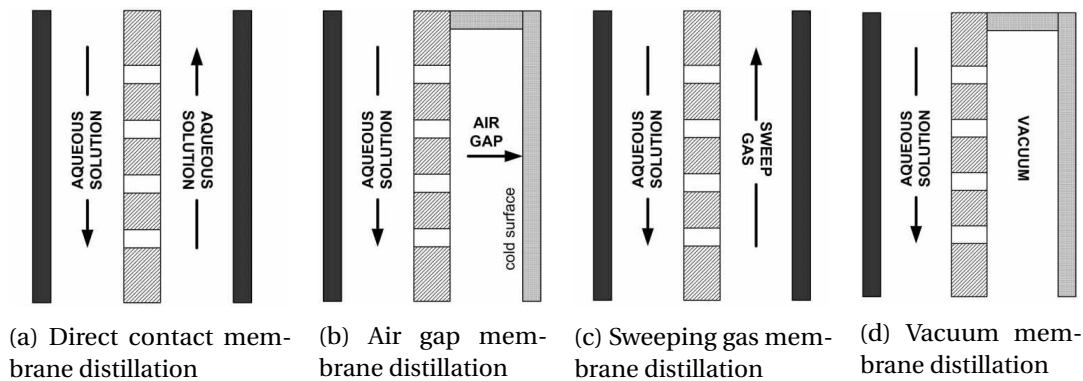


Figure 2.11: Different kinds of membrane distillation. From [37]

Direct contact membrane distillation: Direct contact membrane distillation (abbreviated DCMD) (Figure 2.11a) is the most common way to operate membrane distillation because it is the simplest one [7, 29, 38]. In this configuration, the osmotic side is a condensing liquid or an aqueous solution. The major drawback of this method is that it is the most energy consuming [7]. It is the best choice for application in aqueous solution [29]. Osmotic and thermal membrane distillation are included in this group.

Air gap membrane distillation: Air gap membrane distillation (AGMD) (Figure 2.11b) consists in the presence of a air gap between the membrane and a condensing surface where the liquid will form. The advantage of this technique is it requires less energy than direct contact membrane distillation. Moreover, there is less energy loss. But the problems are it is less efficient than DCMD because air offers a higher resistance to mass transfer. Furthermore, integrating such a condensing surface near the membrane makes the module construction complex. AGMD is mainly used to concentrate non-volatile compounds if there is no need of high fluxes [7, 29].

Sweeping gas membrane distillation: Sweeping gas membrane distillation (SGMD) (Figure 2.11c) uses a cold inert gas to "sweep" the vapour molecules coming from the feed. The gas carries them outside the module to condensate them [7, 29]. Condensation outside the module is consequently the major difference with the two previous distillation method. SGMD manages to combine low conductive loss with low mass transfer resistance [29]. For this reason, SGMD requires less energy compared to DCMD in same time it generates a lower mass transfer resistance than in AGMD [7]. SGMD is mainly used to remove volatile organic compounds from an aqueous solution.

Vacuum membrane distillation: In vacuum membrane distillation (Figure 2.11d), the distillate side is under vacuum and in consequence, the partial vapor pressure is near zero. The condensation occurs outside the module [29]. Given its zero partial pressure in the permeate, its vapor pressure gradient is the highest one of all the membrane distillation possibilities and consequently has the highest mass

transfer [29]. Moreover, there are less heat losses in this system [7]. Unfortunately, this technique is expensive due to the external condensation system [7]. This technique is used to remove volatile organic compounds from aqueous solutions [29].

2.5.3 Mass transfer resistance

The transmembrane flux J can be expressed by Equation 2.8. In this expression, the mass transfer coefficient K can be seen as the global resistance to mass transfer. It results from the combination of three resistances in a series model (see Figure 2.12b):

$$K = \frac{1}{\frac{1}{k_f} + \frac{1}{k_M} + \frac{1}{k_p}} \quad (2.9)$$

where k_f and k_p are the mass transfer resistance related to the boundary layer in feed and permeate side respectively, while k_M is the resistance induced by the membrane. k_f and k_p are related to the mass diffusion in the feed and osmotic side. The solvent has to diffuse from the bulk to the membrane through the boundary layer. The second resistance (noted k_M) is related to membrane diffusion limitations (Knudsen, molecular, surface diffusion) and viscous resistance.

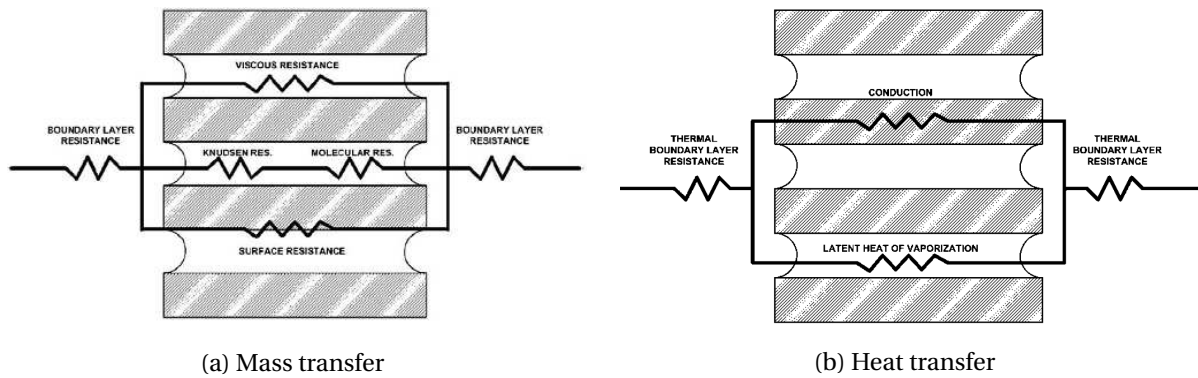


Figure 2.12: Mass and heat transfer resistance model. From [37].

2.5.4 Heat transfer resistance

During membrane distillation, not only mass transfer occurs. There is also a heat transfer which will impact on performance. Similarly to Equation 2.8, heat transfer can be explained by [29]

$$Q = U(T_f - T_p) = \left[\frac{1}{h_f} + \frac{1}{h_m + \frac{J\dot{M}_m \cdot \lambda}{\Delta T_m}} + \frac{1}{h_p} \right]^{-1} (T_f - T_p) \quad (2.10)$$

where Q is the total heat flux ($\frac{W}{m^2}$), U the overall heat transfer coefficient ($\frac{W}{m^2 \cdot K}$), T_f and T_p are bulk temperature in each side, h_f , h_m and h_p are the heat transfer coefficient of feed side membrane and permeate side respectively ($\frac{W}{m^2 \cdot K}$), λ is the molar heat of vaporization ($\frac{J}{mol}$), M_m is the molar mass, ΔT_m is the temperature difference across of the membrane (K). As Equation 2.10 shows it, overall heat transfer coefficient U is also a series combination of several heat transfer resistance, as represented on the Figure 2.12b.

Similarly to mass transfer case, there are two resistances related to heat diffusion (h_f and h_p) while membrane resistance can be decomposed in two contributions acting in parallel.

The first contribution to membrane resistance (h_m) is related to the thermal conductivity through the pore and membrane material. It represents energy that is lost by the system [29]. This conductivity can be lowered by increasing the porosity of the membrane since thermal conductivity of the membrane is one order of magnitude higher than the one of the vapor phase in the pore [7]. Heat loss can be also limited by increasing the membrane thickness in spite of mass transfer reduction [7]. That is why an optimum has to be found. An increase of the temperature and the flowrate also decreases losses by conduction [29]. Generally, this heat transfer resistance is responsible for about 20-50% of the overall heat transfer resistance [29].

The second contribution through the term $\frac{J\dot{M}_m \cdot \lambda}{\Delta T_m}$ is bounded to heat used to evaporate the solvent [29]. The more heat is used for evaporation, the higher mass transfer will be [7].

2.6 Membrane crystallization

In order to recover Na_2CO_3 , membrane crystallization will be used. But before talking more specifically about membrane crystallization, it would be interesting to introduce some basic concepts for a better understanding.

2.6.1 Crystallization principles

Crystallization is a separation and purification technique aiming to generate solid crystals of a solute from a over-concentrated (supersaturated) solution [29, 32, 35]. When a solution has a concentration higher than the saturation concentration, it is called "supersaturated". In this state, solute species are sufficiently abundant and close to cluster together, nucleate and grow as a solid compound [32].

Crystals are characterized by their purity, their morphology, their size distribution and their polymorphism [35]. Polymorphism is the property of a compound to crystallize in different crystal forms [25]. Two polymorphisms are considered, according their physico-chemical properties, as two different compounds [12]. Everyone of these characteristics depends on the relative nucleation and growth rates, which are related to the supersaturation level [14, 29, 35]. They will influence post treatments: filtration, storage, drying, compaction and so on [33], their functionality and their applications [12, 36]. That is why control of the supersaturation will be the main key in every crystallization process.

Figure 2.13 represents a classical phase diagram of a solution in function of the temperature and the solute concentration. Three different areas can be seen on this Figure: an unsaturated zone, a metastable area and a spontaneous nucleation area. The unsaturated zone corresponds to a solution under saturation: no crystallization is possible in this area. The spontaneous nucleation area corresponds to a so supersaturated solution that nucleation occurs spontaneously. In that area, crystals will be created and grow very quickly but without any control [25]. It will lead to impure crystals with inclusions, needle-like shape and small particles [33].

The third region is the metastable area. This area has a kinetic origin. Thermodynamically, crystal is the stable form. But it needs time to form them because of diffusion limitations and the existence of a

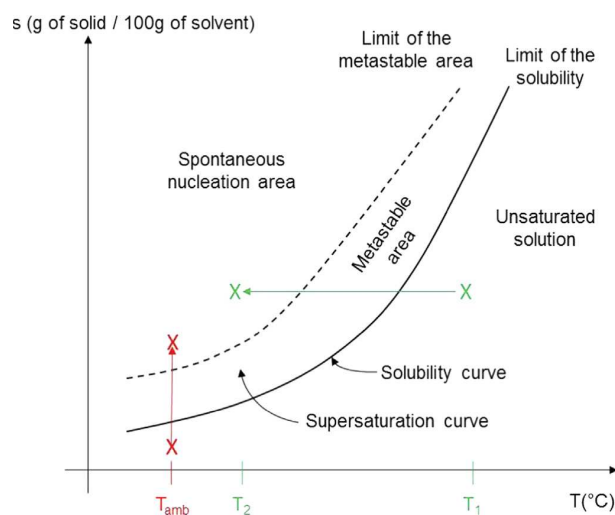


Figure 2.13: Classical phase diagram in function of the temperature and the concentration. Horizontal arrow represents a crystallization by cooling. Vertical arrow represents crystallization by solvent removal. From [35]

critical size below which new nuclei will dissociate rather than growing. The reason is the existence of a free energy barrier to overcome to generate a nucleus. This barrier will be lower when supersaturation level increases, what explains the spontaneous nucleation [29]. Consequently, in metastable area, few nuclei will be create and growth rate will be low. It is in this area that crystallization has to be done [25].

The problem of this metastable area is that limit is not fixed and will greatly depend on the operating condition: solvent, viscosity, temperature, hydrodynamics... [25, 29]. Control of supersaturation level is case dependent. Moreover, there is very few model for nucleation and growing [29].

There is two big ways to operate crystallization and bring solution in a supersaturation state. In one hand, a concentration change can be applied (vertical displacement on Figure 2.13) by solvent evaporation or by precipitants, anti-solvent or chemical addition [29, 32]. On the other hand, the solubility dependence with temperature can be used by cooling or, much more rarely, by heating the solution [29] (horizontal displacement on the Figure 2.13).

The current reference technology for crystallization is the batch stirred tank [35]. Nevertheless it has some drawbacks. Firstly, stirred tank are generally quite big and problems of scale-up appears because hydrodynamics (mixing) and kinetics are modified [29], leading to a bad control of supersaturation condition, an heterogeneous solvent removal or anti-solvent addition point [33]. Therefore, the crystals quality is affected, with a bad reproducibility and finally they do not match the specification [29, 33, 41]. Another problem is bounded to the batch character of the tank which is less practical than continuous conditions. In consequence, researches are done to head for continuous processes. Unfortunately, there are blocking problems preventing their industrial use [35].

Researches are oriented in order to develop an environment favourable to nucleation because it promotes a low nucleation barrier [36]. It is in this context that membrane crystallization intervenes.

2.6.2 Membrane crystallization

Membrane crystallization consists in using the mass transfer generated by a membrane technique to increase the concentration of a solution above its saturation point [29, 31, 36]. The membrane

technique can be membrane distillation [18, 31], reverse osmosis [27] or other membrane techniques. In this thesis, membrane distillation-crystallization will be used. That is why a special look will be devoted to it.

Membrane crystallization differs from membrane distillation (and other membrane concentration techniques by the way) only by the fact that it treats solvent near saturation point and, as a result, can generate crystals [29]. That is why each one of the principles, advantages, inconveniences, and so on, developed in the section 2.5 is applicable here too, particularly less energy consuming because lower temperature needed [32, 33, 41] and the ability to work with low thermal resistant solvent [2, 32].

In order to favour nucleation, membrane crystallization operates in laminar flow condition, which generates few shear stress able to dissociate the nuclei [29]. Moreover, there is a good solution homogeneity due to numerous removal solvent points which the pores are. Other techniques suffer from bad mixing properties and homogeneity problems [41]. But the point where membrane crystallization is very advantageous in comparison with classical stirrer tank crystallizer is that membrane acts as a support for nucleation. Indeed, membrane is a solid media on which solute particles will cluster more easily than in the middle of the solution. Membrane allows to decrease the energy barrier for nucleation and by this way to induce heterogeneous nucleation [14, 29, 32, 33, 36, 41]. The choice of the membrane will be a key parameter: its matter will affect the surface tension for example and help by this way to nucleation [35]. A high surface area and roughness will also enhance nucleation and decrease the induction time (the time between the moment where supersaturation conditions are reached and where the first crystal appears) [35]. The roughness allows to trap solute particles in kinds of cavities, favouring the nucleation [41]. Finally, it has been shown that increasing membrane porosity has a better influence on favouring nucleation than membrane hydrophobicity [36].

Membrane crystallisation also has other advantages. A good supersaturation level can be done thanks to the perfect knowledge of the mass transfer value [14, 33]. It results from this a much better control of crystals properties and quality through a kinetic control [30, 31, 33, 36]. Moreover, membrane crystallisation offers a greater operational and design flexibility than classical method [32]. In one hand, all the classical ways to crystallize (cooling, compounds addition, evaporation) have their membrane counterpart [35]. In the other hand, temperature, feed and osmotic pressure, membrane material, membrane area, feed and osmotic flowrate are as much as control sticks with which it is possible to play [36].

Although it is promising, membrane distillation-crystallization suffers from some problems limiting its industrial use. Firstly, crystals are produced in the membrane. They can accumulate in the fibers and lead to scaling, and even blocking (see Figure 2.14). Some operating conditions such as temperature, fibers size and recirculation rates will greatly have an impact on fouling [29]. Moreover, as for a majority of membrane techniques, there is a lack of long term studies showing the membrane behaviour against the fouling and flux diminution [35]. Another problem will be wetting [33] as membrane choice will favour the crystallization by taking a membrane with a low surface tension with the solute but unfortunately also with the solvent.

Membrane crystallization can be implemented according two ways, represented at the Figure 2.15: either in a hybrid way, either in an integrated way. In an integrated membrane crystallization (Figure 2.15a), the entire crystallization process will occur in the membrane. In the hybrid membrane crystallization (Figure 2.15b), the membrane is followed by a tank in which the crystals growing will occur. The membrane serves to bring the solution to a supersaturate solution, and maybe to generate nucleation. Otherwise, it will occur in the tank too. The hybrid system has some advantages compared to the integrated system. Firstly, as nucleation and growing are sensed to happen outside the module,

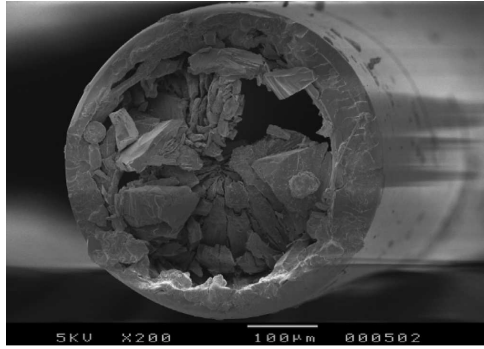


Figure 2.14: Picture of a fiber blocked by scaling. From [35]

it is less subject to fouling. The quantity of the crystals produced can be increased by reducing the temperature of the tank in respect with the contactor temperature [35].

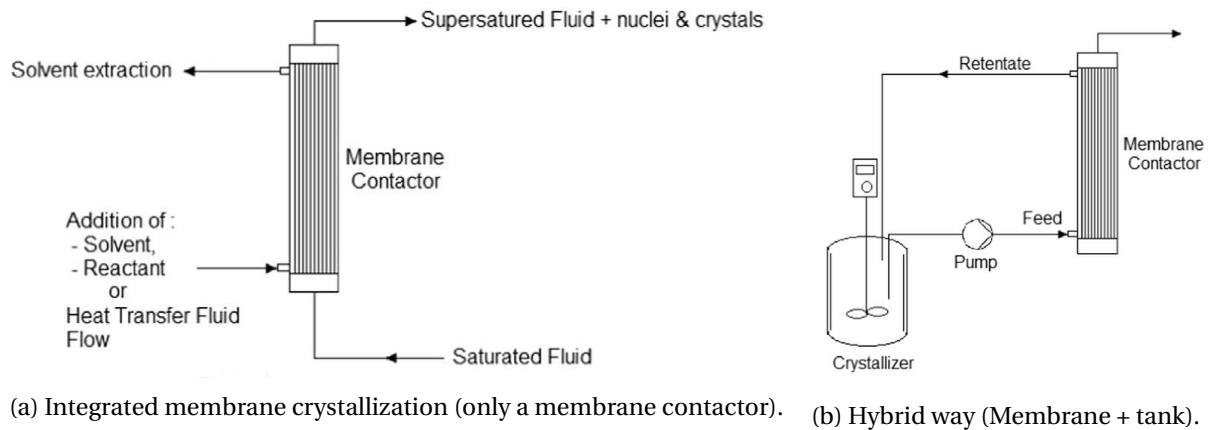


Figure 2.15: Different ways to operate membrane crystallization. From [35].

Membrane crystallization are applied in some fields such as protein purification and crystallization [12, 33], salt crystallization [12], water desalination [30, 36], pharmaceutical compounds production [33] and recovery of compounds present in waste stream [33].

Chapter 3

Objectives of the thesis

3.1 Overall objective of the research project: CO_2 capture by using membrane technology

In the previous section, potential of membrane techniques, especially in term of energy saving, has been shown compared to classical solution. That is why it could be interesting to use them in an environmental goal, as CO_2 capture. This Master thesis is part of a big project developed by the researcher Israel Ruiz Salmón and his promoter, Patricia Luis [4]. The flowsheet of the integrated membrane process of the PhD is available at the Figure 1.1 In this section, each one of the big steps (membrane absorption, nanofiltration and membrane distillation crystallization) will be detailed.

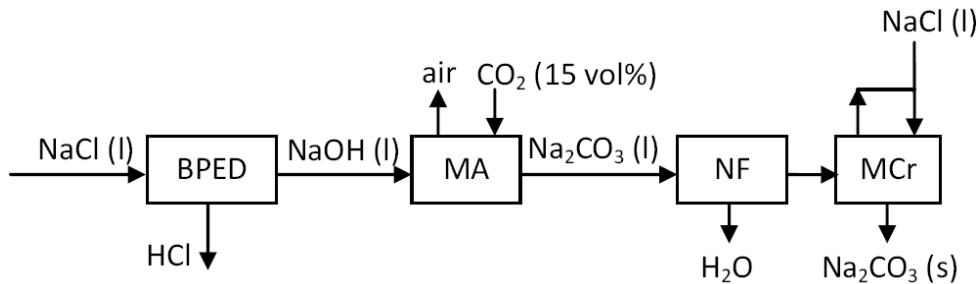
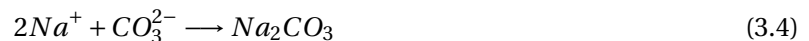


Figure 3.1: Flowsheet studied in the framework of Israel Ruiz Salmon's PhD [4]. The flowsheet uses only membrane contactors and will allow to capture CO_2 . BPED: bipolar electro dialysis. MA: Membrane absorption. NF: Nanofiltration. MCr: Membrane crystallization.

The first step of the process is the membrane absorption. The absorption is done with a $NaOH$ solution, flowing in counter-current with respect to the flue gas, as absorbent. The OH^- ions of the solution will chemically capture CO_2 by the following steps [14]:



It will be the predominant schema provided that pH will be higher than 8 [11], which will probably be the case due to the high alkaline potential of $NaOH$. Otherwise some HCO_3^- will be produced.

The choice of the membrane absorption rather than a classical absorption is due to the numerous advantages membrane absorption has: higher surface area so more exchange possible [2], less energy required, no emulsion, no foaming, no entrainment [11], less solvent need [2], operational flexibility especially for the flow rates [13], compactness, and so on. As far as the choice of the $NaOH$ as absorbent is concerned, motivations are, in one hand, a Na^+ source for the Na_2CO_3 production and, in the other hand, the fact it showed high removal efficiency in gases containing at least 10% CO_2 [12, 14]. The exhaust gas to treat has a CO_2 concentration of 15% vol, which is the typical CO_2 composition of flue gas of combustion plant [17]. The Na_2CO_3 formed is in an aqueous form and very diluted [4].

The nanofiltration step aims to concentrate the solution stream leaving the membrane absorption. By the way of membrane media, water will be removed by crossing the membrane thanks to the application of an external pressure. It has to bring the Na_2CO_3 concentration close to saturation [4].

The last step, membrane crystallization, aims to crystallize Na_2CO_3 . Solvent removal will be carried out by an osmotic membrane distillation. The partial pressure gradient will be generated by a highly concentrated $NaCl$ solution, flowing the shell side in counter-current with respect to the feed flow. Residual heat of the process can be used to strengthen the partial pressure gradient and remove more water [4].

The Na_2CO_3 crystals can be used in different applications, such as food industry [12, 18], glass industry [12, 18], cement industry [4, 12], ceramic industry [4], laundry detergent and cleaning products [18]. The final application will greatly depend on the crystal purity [12].

3.2 General and specific objectives of the Master thesis

This Master thesis will mainly focus on the last step of the process, namely the membrane crystallization. The objective is to characterize the membrane distillation-crystallization process and to obtain crystals as final product. In the end it will lead to establish if the entire process for CO_2 capture is viable or not.

More specifically, objectives are:

- To characterise fluxes in function of Na_2CO_3 concentration in order to be able to calculate the membrane area needed in a concrete case. It can also be interesting in order to determine in further research if nanofiltration step can be replaced by membrane distillation or if both can be associated in an optimal way.
- To study the effects of the temperature if there are interests to use extra energy to improve the performance of the system. especially the effect of osmotic temperature.
- To analyse the membrane distillation-crystallization performance and to characterize crystals purity. Water content, chloride content and quantity produced will be studied because it will impact the post-treatment process and the industrial utilization of the crystals
- To study scale-up possibility by adding a second module in series. The idea is to see if the transmembrane flux is affected by the change of scale.

Chapter 4

Materials and methods

In order to study the membrane-crystallization step of the process, several experiments were done. This chapter will present the different used equipments, the different measurements done during experimentations and the different set-ups in which they were used. The different technical operations such as preparing the solution or making the measurements will also be explained.

4.1 Chemicals and equipments used

4.1.1 Chemicals

Three main compounds will be used during the experiments:

- Na_2CO_3 (Anhydrous, Analar Normapur, 99.5% purity, produced by VWR), the solute of the feed solution
- $NaCl$ (Analar Normapur, 99.5% purity, produced by VWR), the solute of the osmotic solution
- Deionized water (Electrical resistivity= $18.2M\Omega \cdot cm^{-1}$), the solvent of both feed and osmotic solutions.

4.1.2 Equipments

Membranes

The crystallization step is done by the way of a membrane contactor. The one used in the lab is a *Liqui-Cel®2.5x8Extra-flow* contactor. Its characteristics are given in Table 4.1.

The membrane cell have two pairs of inlet-outlet: one for fibers side and the other one for the shell side, in order that the two flows coming do not mix together. These flows come and leave the module by plastic pipes. Several peristaltic pumps (Masterflex) are in charge to make circulate the flows at the desired flowrates.

Module configuration	Hollow fibres
Housing	Polycarbonate
Potting	Polyurethane
Membrane type	Celgard ®X50-215 Microporous Fiber
Membrane material	Polypropylene (hydrophobic)
Shell side volume	approx. 400 ml
Fibre side volume	approx. 150 ml
Porosity	40%
Effective pore size	0.04 μm
Inner/outer diameter	220 μm / 300 μm
Wall thickness	40 μm
Active surface area	1.4 m^2
Number of fibers	approx. 11 000
Brust strength	27 bar
Contact angle	112°
Max. Operating temperature	70°C at 1 atm

Table 4.1: Technical informations about Liqui-Cel®2.5x8Extra-flow membrane. From [34]

Other equipments

An important operating condition in some experiments is temperature. That is why cooling and heater bathes will be used to regulate the temperature of the flows. The cooling bath is made by adding ice in a water bath in a sufficient quantity. Thermometers will serve to measure the temperature during the experiment.

Manometer will be used to measure the pressure of the system. When membrane is about to block, pressure in the system will take off. It is a safety measure to prevent damages related to blockage.

Other classical laboratory devices will be used as balance, thermometers, volumetric flasks, graduated cylinders, beakers and watch glasses. Membrane filters and a vacuum pump were also used to filtrate saturated solutions as it will be explained further.

4.1.3 Preparation of the solutions

During the experiments, high volumes (3 – 4l, even 6l in the 2 membranes series set-up) of highly concentrated (until 300 $\frac{g}{l}$) solutions had had to be used. The reason is that small volume solution will be more affected by volume and concentration changes, as it is illustrated in Table 4.2. It is problematic because high concentration changes means high driving force changes during the experiment and the results obtained during the experiment will not be reliable anymore.

NaCl solution

Solutions are made by following the procedure detailed in Table 4.3. However, in some cases, an old solution was reused and making solution by recycling an old one is a little bit different from making a new one. At the end of the previous experiment, a *NaCl* solution with a higher volume but with concentration lower than the desired one is obtained. Salt has to be added to the solution as well as its

	<i>NaCl</i>		<i>Na₂CO₃</i>	
initial volume (<i>l</i>)	1	3	1	2
initial concentration ($\frac{g}{l}$)	300	300	150	150
final volume (<i>l</i>)	1.27	3.27	0.73	1.73
final concentration ($\frac{g}{l}$)	236.2	275.2	205.5	173.4
concentration change (%)	-21.22	-8.26	+37.00	+15.60

Table 4.2: Example of concentration variation during a typical experiment for different volume. Average flux is $1.61 \frac{ml}{m^2 \cdot min}$, membrane surface is $1.4m^2$ and experiment time is $2h$. Percentage concentration change is given by $\frac{C_f - C_0}{C_0} \cdot 100\%$.

Step	Action
1	Filling the flask with a little of pure water
2	Adding the solute
3	Filling the flask with water until a little bit under the graduation Rinsing watch glass and funnel to remove stuck solute
4	Mixing
5	Filling with water until the graduation

Table 4.3: Classical methodology to prepare the solutions.

volume has to be decreased. Therefore some losses are unavoidable. The following approach describes how solutions were made.

A new solution of volume V_{new} and concentration C_{new} is wanted. An old solution of concentration C_{old} whose volume is higher than V_{new} is used to make it. Therefore, in order to limit losses, the highest volume V_{old} possible is taken but by keeping a margin to be able to add water to rinse the equipment and reach the graduation. For instance, if $V_{new} = 1l$, a volume $V_{old} = 0.9l$ or $0.95l$ will be taken. The quantity of solute to add m_{added} is given by:

$$m_{added} = C_{new}V_{new} - C_{old}V_{old} \quad (4.1)$$

Preparing the solution will be similar to the procedure described in Table 4.2 with some little changes. First in step 1, it is a little of the old solution that is used to fill the flask. Then in step 3, the rest of the old solution is used before continuing with water.

Na₂CO₃ solution: normal case

Contrarily to *NaCl* solutions, *Na₂CO₃* solutions will be more concentrated and have a lower volume than the desired solution. Generally, the whole solution can be recycled (= V_{old}). Water is just added to obtain the final volume with maybe a very low *Na₂CO₃* addition determined by Equation 4.1 to reach accurately the desired concentration. But simple dilution (without *Na₂CO₃* addition) will be often sufficient.

An aspect encountered by making the solutions, especially the *Na₂CO₃* ones, is that their dissolution is exothermic. Therefore, the temperature was often too high whereas experiments are done at room temperature. That is why solutions were prepared one day before the experiment.

Na_2CO_3 solution: saturated solution

A particular case will be the production of saturated solution for the study of crystallization. The way to make the solution described above is problematic because the Na_2CO_3 saturation is very dependent on temperature. Therefore, the next day, when temperature had decreased, crystals were present again, so heating and mixing in the same time were required. At the end, either solution was too poorly concentrated and it needs a lot of time before crystallization occurred, either crystals were still present in the solution and blocked quickly the membrane after some minutes.

To solve this problem, a very supersaturated solution was prepared. Crystals were formed during the night. Just before the experiment, solutions were brought around $20^\circ C$ and mixed to dissolve crystals during 1 hour. As crystals were logically still present and it was not possible anymore to dissolve some more, the solution was supposed to be saturated. To remove crystals, filtration was applied to the solution. A little water ($10ml$) was added to dissolve a little the solution to avoid too quick formation of crystals.

4.2 Experimental set-ups

4.2.1 First set-up: concentration influence

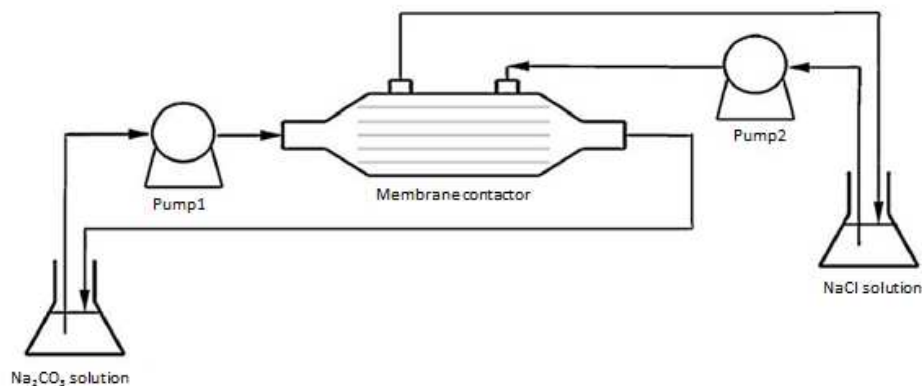


Figure 4.1: Flowsheet of the first set-up. Adapted from [32]

The first set-up was mainly used to study the dependence of the transmembrane flux with feed and osmotic concentration. It is the simplest set-up and is represented in Figure 4.1. The Na_2CO_3 enters in the fibers of the contactor and $NaCl$ in the shell side, in a counter-current way. Each solution goes back then in its tank.

The pumps provide flowrates for the osmotic flow ($NaCl$) at $450ml/min$ and for Na_2CO_3 flow at $300ml/min$. These flowrates are used because Janssens [2] has studied the effect of flowrates and saw that beyond $300ml/min$, no mixing of solutions was required because the turbulence of the flow was sufficient to ensure a correct one. Moreover, putting these flowrates also allows to avoid polarization in the membrane [2].

Two series of experiments were done with this set-up and are developed in Table 4.4.

N°	Na_2CO_3 ($\frac{g}{l}$)	Na_2CO_3 T (°C)	$NaCl$ ($\frac{g}{l}$)	$NaCl$ T (°C)
1	0-10-35-75-150	20	300	20
2	0-10-35-75	20	200	20
3	150	20	300	20

Table 4.4: Experimental conditions used with the first set-up. Osmotic volume is 3l, feed volume 2l. Feed flowrate is $300 \frac{ml}{min}$. Osmotic flowrate is $450 \frac{ml}{min}$. The set of experiments n°3 is different from the n°1 because water and $NaCl$ were added to keep concentration constant.

The first series aims to study the effect of the feed concentration on the flux. $300 \frac{g}{l}$ of $NaCl$ was taken to have the highest driving force. Similar experiments have already been done by Janssens [2]. However, he limited his study to concentration above $100 \frac{g}{l}$. Realising these experiments at lower concentration is motivated by a possibility to shift the nanofiltration step of the process described in Section 3.1 by a membrane distillation.

The second series of experiments are done with a lower concentration of $NaCl$ in order to see the influence of the osmotic concentration on the flux. Moreover, using a lower concentrated $NaCl$ solution would maybe lead to a more efficient water removal in the sense a bigger part of the driving force will be used to generate the flux. In that case, although high $NaCl$ concentration is more effective, using lower $NaCl$ concentration would be justified by a better use of the membrane technology.

In two first series, assumption was done that concentration variations during the experiments do not affect too much the measured fluxes. The third set of experiments aims to check if this assumption is valid or not by keeping both concentrations constant during the experiment. It will be done by regularly adding water and $NaCl$ to compensate feed concentration increase and osmotic concentration decrease respectively.

4.2.2 Second set-up: temperature influence

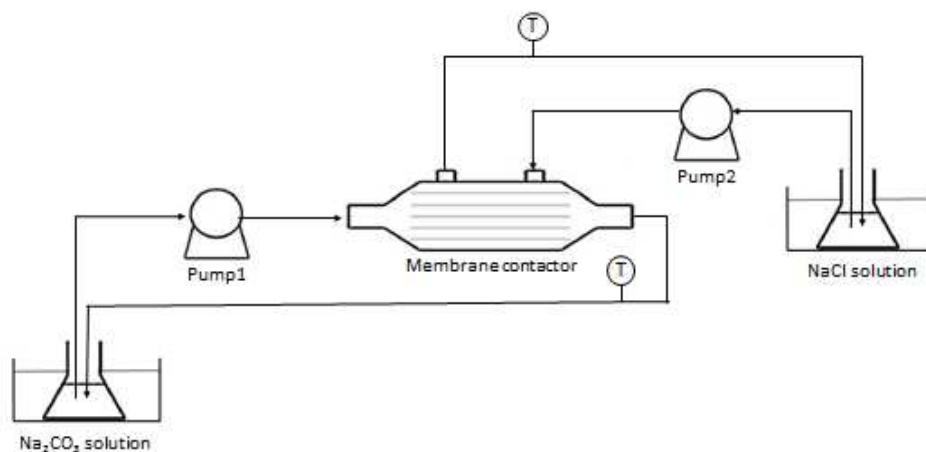


Figure 4.2: Flowsheet of the second set-up. Adapted from [32].

The second set-up targets to study the influence of the solutions temperature on the flux. The flowsheet is represented on Figure 4.2. The difference with the first set-up is that feed and osmotic

solutions are placed in a heat exchanger to heat or cool them according to the need. Temperature is measured in each solution to know the inlet temperature and on-line at the outlet of the contactor. By this way, temperature variation in the contactor can be known.

Two series of experiments were done with this set-up. They are presented in Table 4.5.

N°	Na_2CO_3 ($\frac{g}{l}$)	Na_2CO_3 T ($^{\circ}C$)	$NaCl$ ($\frac{g}{l}$)	$NaCl$ T ($^{\circ}C$)
1	150	20	300	20-25-30
2	150	40	300	20-30-40

Table 4.5: Experimental conditions used with the second set-up. Osmotic volume is 3l, feed volume 2l. Feed flowrate is $300 \frac{ml}{min}$. Osmotic flowrate is $450 \frac{ml}{min}$.

In the first series, osmotic temperature will be higher than the one of the feed. The temperature gradient is therefore negative and opposes the concentration gradient. The increase of the osmotic temperature was motivated due to the decrease of the heat losses [30], which is a big problem in membrane distillation. The osmotic temperature was also be increased in an experimental goal: it could be used in experiments aiming to control crystallization thanks to a lower water flux induced by the decrease of the partial pressure gradient.

The second series of experiments repeats the same experiments as the first one, but with an higher feed temperature in order to see its effects. Furthermore, it would be nice to characterise the flux at higher feed temperature in case the incoming stream was not at room temperature. Finally, crystallization at $40^{\circ}C$ gives crystals with less water content than at $20^{\circ}C$ (see Figure 4.8). Knowing the flux at this temperature will allow a better prediction of the results.

4.2.3 Third set-up: crystallization

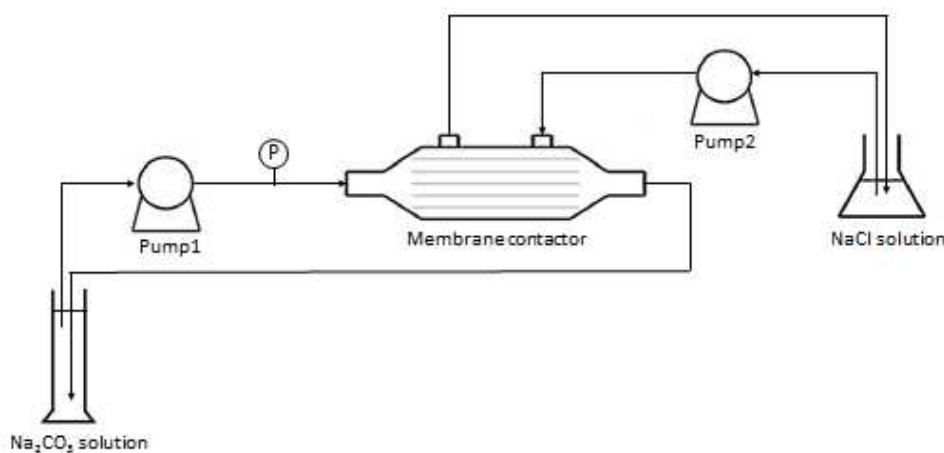


Figure 4.3: Flowsheet of the third set-up. Adapted from [32].

The third set-up was thought to try to favour crystallization. In this goal, the shape of the feed tank was changed. The idea is that the crystals arrive in the bottom and stay there. The feed solution was taken in the upside part without entraining crystals (see Figure 4.4). A long cylindrical shape seems

suitable to carry out such a function.



Figure 4.4: Disposition of the tubes in the feed column. The upper tube brings the feed solution towards the membrane. The lower one brings back the solution with potentially crystals.

Another change with respect to the other set-ups is the addition of a manometer just before the module. The only reason of this addition is to anticipate a blocking. When pressure starts to take off, it means that the flow has a lot of difficulties to cross the module, the pump has to give more pressure in order that the solution continues its path. When pressure becomes too high, experiment was stopped to prevent total blockage, which risks to damage the membranes. Moreover, from a technical point of view, it is easier to clean the membrane when the fibers are partially blocked because the water can easily flow.

Two series of experiments were done with this set-up and are described at Table 4.6.

N°	Na_2CO_3 ($\frac{g}{l}$)	Na_2CO_3 T (°C)	$NaCl$ ($\frac{g}{l}$)	$NaCl$ T (°C)
1	215	20	300-250-200	20
2	210	20	300	20

Table 4.6: Experimental conditions used for the third set-up. Osmotic volume is 3l, feed volume 2l. Feed flowrate is $300 \frac{ml}{min}$. Osmotic flowrate is $450 \frac{ml}{min}$.

The first set of manipulations was devoted to try to obtain crystals without blocking the membrane. Blocking was suspected to occur because of a too high supersaturation level in the membrane. The objective is therefore to limit it by decreasing the driving force to allow a better control. Supersaturation control was done by decreasing the osmotic concentration.

The goal of these experiments is to see in a first time how long the system can last and produce crystals before blocking apparition. Furthermore, flux characterization was done in order to be able to

estimate the surface area needed to treat any incoming flow in further applications.

The second set aims to estimate the crystals production during one experiment from a solution whose concentration is accurately known. During this experiment, *NaCl* is added at regular time interval to kept the osmotic concentration constant.

4.2.4 Fourth set-up: two membranes in series

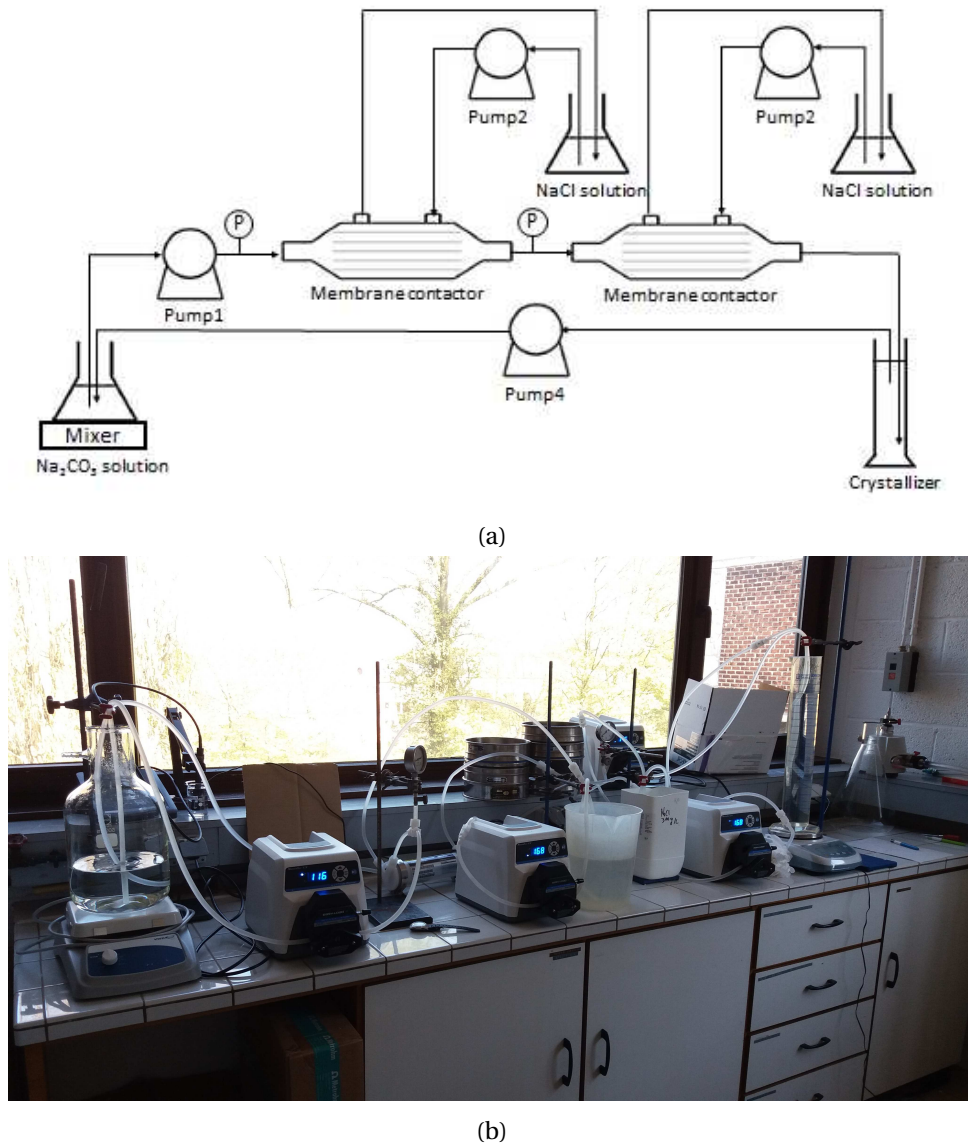


Figure 4.5: Flowsheet of the fourth set-up (schema and experiment picture). Schema adapted from [32].

The last set-up consists in putting two modules in series to study the scale-up possibility of the membranes (see Figure 4.5). There is one osmotic tank by module. The advantage of such a disposition is that it is possible to have a different osmotic concentration for each membrane, and therefore a different driving force. For example, a high driving force could be used in the first module to concentrate

the flow and a lower one in the second to control crystallization.

An alternative set-up (see Figure 4.6), without the crystallizer, was also used. Moreover, mixers were added below the $NaCl$ tank in order to mix the $NaCl$ added with the solution.

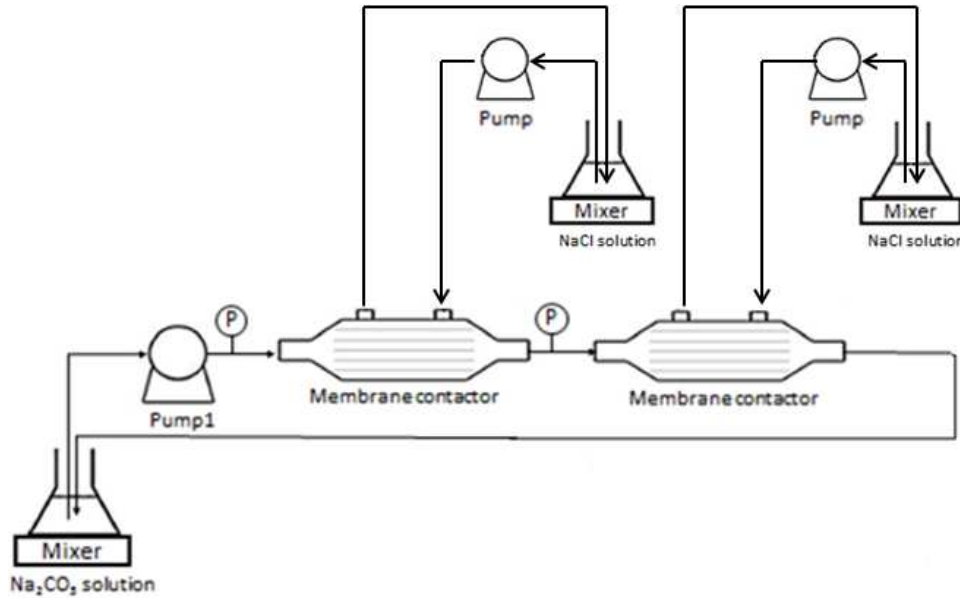


Figure 4.6: Alternative flowsheet of the fourth set-up. Adapted from [32].

Two kind of experiments were done with this set-up (see Table 4.7).

N°	Na_2CO_3 ($\frac{g}{l}$)	Na_2CO_3 T ($^{\circ}C$)	$NaCl$ ($\frac{g}{l}$)	$NaCl$ T ($^{\circ}C$)
1	210-216	20	300	20
2	150	20	300	20

Table 4.7: Experimental conditions used for the fourth set-up. Osmotic volume is $2 \times 3l$, feed volume $4l$ in the first series, $2l$ in the second. Feed flowrate is $300 \frac{ml}{min}$. Osmotic flowrates is $450 \frac{ml}{min}$.

The first series was done with the set-up on the Figure 4.5 in order to obtain crystals in a continuous way. The problem encountered in the previous set-up was that by recycling the feed constantly, concentration increases all the time until membrane blocks. It is not the way the system was designed to work in the industry. It is a continuous system: concentration are sensed not to change with time. To have a similar case experimentally, water was added in the feed solution to keep concentration more or less constant. The amount of water to add was computed on the basis of the results of the previous set-up.

The second series was done with the set-up of the Figure 4.6 to see if using two modules gives the same flux as using one. Water and $NaCl$ will be added to the feed and the osmotic solution each 5 minutes to keep the concentration constant. Amounts added was calculated on the basis of the results of a similar previous experiment. The results were compared with the ones obtained for the third set of experiments of the first set-up (see Section 4.2.1).

4.3 Experimental procedure

Two different kinds of experiments were done: the ones to characterise the flux and the ones to characterise the crystallization.

4.3.1 Flux characterization

Experiments concerned by this procedure are the ones described in Sections 4.2.1, 4.2.2 and 4.2.4 (only the second one in Table 4.7). At the beginning and during the experiments, the feed solution was weighed and concentrations of both feed and osmotic solutions measured. The weighing is done to compute the transmembrane flux of the membrane (see Section 4.4.2). The concentration is measured only to have an idea of its evolution. The first 10 minutes of the experiments were devoted to fill the membrane and to remove air from the system. After the 10 minutes, experiment was stopped to weigh the feed solution and measure concentration of every solution. The weighing was done by clamping the tubes, removing them of the solution and carrying out the weighing.

The weighing procedure was repeated every 15-20 minutes. Seeing as the system is stopped, hydrodynamics will be affected. To limit the impacts, operating time has to be much longer than the time during which experiment is stopped. The weighing procedure lasts more or less one minute. Experiments done by R.Janssens[2] showed that the weighing procedure did not influence the results provided that the time between two measurements was superior to 10min. Therefore, a time interval of 15-20 min between two measurements was chosen rather than 10 min to have a safety margin.

The total experiment duration was about 1h30-2h so that 5-6 measurements were taken. In the case of crystallization experiment, the experiments were run until blockage. The membrane is then cleaned by rinsing it with pure water. Then the water is removed by blowing air during several minutes in the membrane.

4.3.2 Crystallization

When concentration was close of saturation (more than $210 \frac{g}{l}$), as it was the case for experiments described in Section 4.2.3, the experiment was not stopped and weighing was done on-line, the tank being constantly on the balance. The tubes were in this case left in the solution. The reason is that even when the experiment is stopped, there is still some flux in membrane. In consequence, supersaturation can be locally reached and crystals can be formed and block the membrane.

Measurements were generally done every 15-20 minutes as the previous case but as the experiments were not stopped, they could be done more often. By the way, measurements were done every minute for the experiment 2 in Table 4.6. However, as the weigh value displayed by the balance is varying, it is difficult to have an accurate measure. That is why a mean of several (between 3 and 7) values taken at different time centred on the measurement time was done. For example, if a measurement has to be done after 20 minutes, weigh values will be taken at 19 min 30 seconds, 19 minutes 40 seconds, 19 minutes 50 seconds and so on each 10 seconds until 20 minutes 30 seconds.

Another interest of these experiments was to observed if there is crystals formation or not. It was simply done by looking in the column if there are any. It was also needed to be careful the feed tube (the one which is the closest of the surface) was always in the solution. It was sometimes necessary to put it a little bit lower during the experiment. Finally, a particular attention was paid on the manometer

to prevent scaling.

Finally, the ending procedure differs from the previous part by the fact the contactor could be blocked. First of all, it is better to use hot water (34 – 40°C) because Na_2CO_3 has an higher solubility at these temperatures. If the membrane is blocked and high flows are used, there are risks of breaking. Therefore, both flowrates were put at $100 \frac{ml}{min}$ by prevention. If the fibers were blocked, feed pump was turned off. An attempt to turn it on was done every 2 minutes. Once the feed pump was working correctly, a flow shock was done. Then the classical cleaning procedure was applied.

4.4 Characterization and analyses

4.4.1 Conductivity meter

A conductivity meter was used to know the concentration of both solutions during the experiments. It is important especially to make the new solutions for the next experiment (see Section 4.1.3).

The conductivity meter gives the conductivity of the solution at 20°C. When temperature is different of this temperature, the device uses a linear correction (2.07%/°C) of the value of conductivity to show the one at 20°C. The conductivity meter is equipped with a Pt1000 probe which gives temperature of the solution.

In order to determine the concentration of an unknown solution of $NaCl$ or Na_2CO_3 , a calibration curve was made by measuring the conductivity of several solutions with a known concentration (see Figure 4.7). Referring this curve will then allow to find the concentration of the unknown solution.

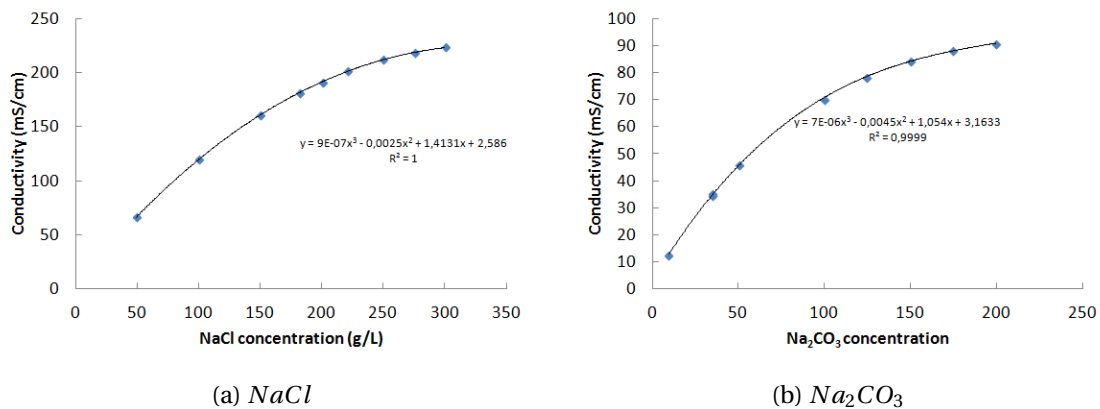


Figure 4.7: Calibration curves of the conductivity meter.

4.4.2 Flux measurement

In nearly all the experiments, flux was characterized. The objective is to establish a relationship between transmembrane flux and operating conditions (flows concentration and temperature). These data could be used to size a higher scale plant for example.

As it was said in the Section 4.3, feed solution was weighed every 15-20 minutes. Only water is assumed to cross the membrane. In reality, some ions (Cl^- , CO_3^{2-}) do too, but in very negligible amount, as it will be seen in the Section 5.3.4. Therefore, the decrease of the feed weight during time is only due to water removal by the membrane. The flux J is then given by the relationship [14]:

$$J(t_i) = -\frac{1}{A} \left. \frac{dV_f}{dt} \right|_{t_i} \approx -\frac{1}{\rho_{water} A} \frac{m_f(t_i) - m_f(t_{i-1})}{t_i - t_{i-1}} \quad (4.2)$$

where A is the membrane surface (m^2), V_f the feed volume (ml), m_f the feed m (g), ρ_{water} is the water volumetric mass density ($\frac{g}{ml}$) and t is the experimental time (min). The index i refers to the measurement number.

The curves transmembrane flux in function of a parameter (temperature, concentration) were established by taking the average of the last 4 fluxes of the experiment. The reason is that the flux decreases quickly at the beginning of the experiment, then stabilizes. In the event that several experiments were carried out in the same conditions, average is done on the basis of the 4 last measurements of each one of them. Finally, standard derivation is computed to have a confidence interval (in the form of error bars) for the values measured.

4.4.3 Mass transfer coefficient

Mass transfer coefficient K presented in Equation 2.8 was computed by the way of the following model:

$$K = \frac{J_{avg}}{p^{vap}(T_f) a_f - p^{vap}(T_p) a_p} \quad (4.3)$$

with all factors expressed in SI units ($\frac{m^3}{m^2 \cdot min}$ for J_{avg} , Pa for p^{vap}). p^{vap} and activities calculations are based on mathematical models detailed in Appendix A.

For experiment with the second set-up, temperature will be different between the inlet and the outlet at each side due to the heat exchange. That is why to be able to use Equation 4.3, a logarithmic mean of temperature (T_{lnmean}) at each side will be used for T_f and T_p .

$$T_{lnmean} = \frac{T_o - T_i}{\ln(T_o) - \ln(T_i)} \quad (4.4)$$

where T_i and T_o are the temperature at the inlet and the outlet respectively ($^{\circ}C$).

4.4.4 Average and standard derivations

During a single experiment, several values of flux and mass transfer coefficient were measured (one every 15-20 minutes). In order to plot flux or mass transfer coefficient in function of the experimental parameters, average and standard derivation of the experiments values will be computed. Average values (J_{avg} and K_{avg}) are computed thanks to the following relationships:

$$J_{avg} = \frac{1}{N} \sum_{i=1}^N J_i \quad (4.5)$$

$$K_{avg} = \frac{1}{N} \sum_{i=1}^N K_i \quad (4.6)$$

where N is the number of experimental measurements taken into account (generally, the last four ones)

In order to have a confidence interval around the average values obtained, standard derivations (J_{std} and K_{std}) are computed by the equations:

$$J_{std} = \sqrt{\frac{1}{N} \sum_{i=1}^N (J_i - J_{avg})^2} \quad (4.7)$$

$$K_{std} = \sqrt{\frac{1}{N} \sum_{i=1}^N (K_i - K_{avg})^2} \quad (4.8)$$

These values are represented on the graphs in Chapter 5 in the form of error bars.

4.4.5 Total water fraction

Na_2CO_3 crystals can have several forms in function of the temperature at which the crystallization is done, as shown at Figure 4.8. They can exist pure or in the form of hydrates. A procedure was developed to characterized under which form the crystals produced during the experiment are.

Firstly, an empty watch glass is weighed (w_{plate}). Crystals were removed from the solution by filtration. Their surface was dry thanks to a piece of paper to remove water droplets on the surface. The crystals are put on the watch glass and the set is weighed (w_{ini}). Crystals were let dry at free air during 24h. Then they were put in an oven at 105°C during 4h. Crystals were from this point forward considered in its purest form (Na_2CO_3), all the water they contained were removed and evaporated. The anhydrous crystals are weighed ($w_{anhydrous}$). The total water fraction of the crystals, TWF, is given by:

$$TWF = \frac{w_{ini} - w_{anhydrous}}{w_{ini} - w_{plate}} \cdot 100\% \quad (4.9)$$

Theoretical total water fraction of each form of Na_2CO_3 crystals is given at Table 4.8.

Crystals	Na_2CO_3	$Na_2CO_3 \cdot H_2O$	$Na_2CO_3 \cdot 7H_2O$	$Na_2CO_3 \cdot 10H_2O$
TWF (%)	0	14.52	54.31	62.94

Table 4.8: Total water fraction of Na_2CO_3 crystals.

4.4.6 Quantitative analysis of Cl^- content by Charpentier-Volhard's method

To calculate the water transmembrane flux, it was assumed that only water crosses the membrane. However, there also exists a concentration gradient for ions species. For example, Cl^- , present in large amount in the osmotic solution, was not present in the feed. It could be expected that some Cl^- ions goes from the osmotic to the feed. By the way, Luis et al. [14] showed it was the case and some Cl^- ions were found in crystals. Knowing the amount of Cl present in the solutions and in the crystals from which they are formed can therefore be interesting.

The method used to determine the amount of Cl present is the Charpentier-Volhard's method. The principle is based on a back titration method. In a solution sample, a large excess known amount of $AgNO_3$ is added. All the Cl^- ions contained in the solution precipitate in $AgCl$ because of their poor solubility [42].



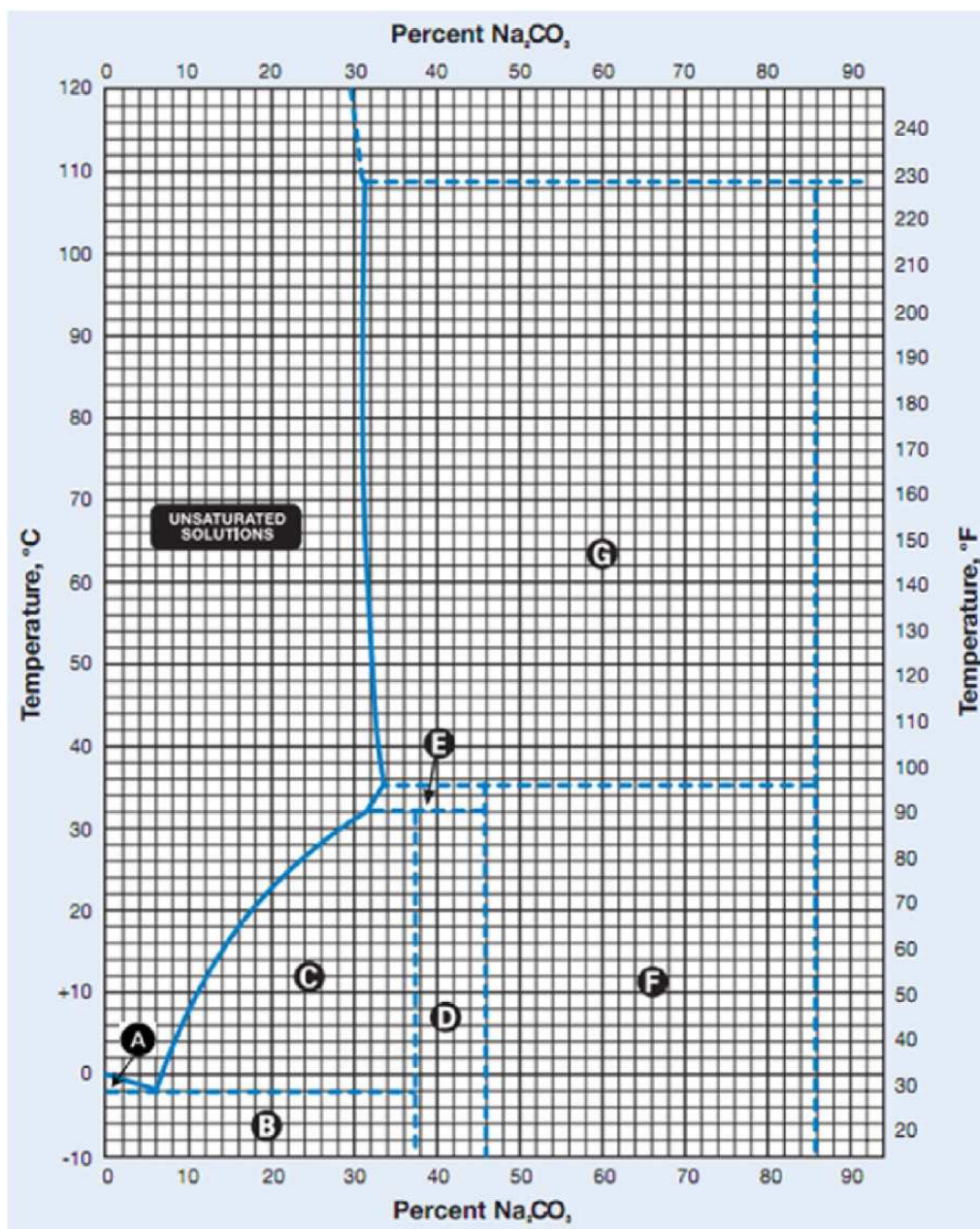


Figure 4.8: Phase diagram of Na_2CO_3 . From [18]. Area A: Ice. Area B: Ice+ $Na_2CO_3 \cdot 10H_2O$. Area C: $Na_2CO_3 \cdot 10H_2O$. Area D: $Na_2CO_3 \cdot 10H_2O + Na_2CO_3 \cdot 7H_2O$. Area E: $Na_2CO_3 \cdot 7H_2O$. Area F: $Na_2CO_3 \cdot 7H_2O + Na_2CO_3 \cdot H_2O$. Area G: $Na_2CO_3 \cdot H_2O$. Area H: $Na_2CO_3 \cdot 7H_2O + Na_2CO_3$. Area I: Na_2CO_3 .

The solution is filtrated to remove the formed solid. As $AgNO_3$ has been voluntary added in excess, it remains Ag^+ ions in the solution. This quantity will be measured by a titration with $KSCN$ [42].



An indicator containing Fe^{3+} ions was used to see when there are no more Ag^+ ions. Indeed, SCN^- ions will prefer reacting with Ag^+ ions rather than with Fe^{3+} . When there are no more Ag^+ ions, SCN^- ions will form a complex with Fe^{3+} . Its particularity is that it will induce a radical change of colour of the solution, becoming dark red. The colour change highlights the moment there are no more Ag^+ ions [42].

The number of moles of Cl^- present is given by:

$$n_{Cl^-} = n_{AgNO_3} - n_{KSCN} \quad (4.12)$$

where n_{AgNO_3} is the number of moles of $AgNO_3$ added before the titration, n_{KSCN} the quantity of $KSCN$ added during the titration. To obtain the concentration of Cl^- that was previously in the solution, it requires to divide by the initial sample volume and take into account the potential dilution factor.

In case of crystals, it just needs to dissolve a known quantity of crystals to make a solution. Then, it is the same procedure as for a solution.

Several solutions and crystals coming from these were analysed. Some of them were reused several times to see if reuse of solutions is not problematic.

4.4.7 Mass production estimation

It can be interesting to have an idea of the capacity of the membrane technology to produce crystals, for instance by weighing the quantity of crystals produced. However, it is very difficult to weigh all the crystals produced because a lot of them are in the module and block it. An alternative method has to be found.

The method used to estimate the crystals production in the second set of experiments devoted to crystallization study (see Table 4.7) was based on a difference of concentrations between the one it should be obtained and the saturation one. Theoretical concentration is computed on the basis of the flux measured during the experiment, providing that initial concentration is accurately known.

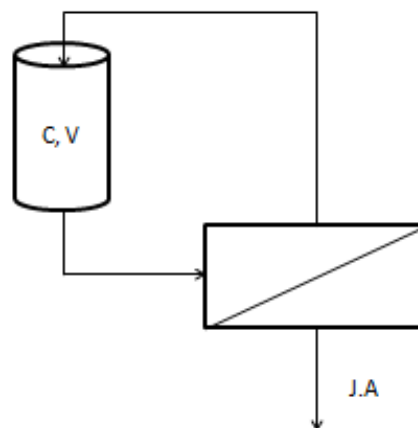


Figure 4.9: Simplified schema of the feed tank connected to the membrane. V is the volume of the feed solution, C its concentration, A is the membrane area and J the transmembrane flux.

Figure 4.9 shows a simplified schema of the set feed tank plus membrane. By the way of a Na_2CO_3 mass balance and a volume balance, volume and concentration evolution can be followed. The volume

V_f of the feed solution only varies because water is removed by the membrane. The mass of Na_2CO_3 $m_{Na_2CO_3}$ does not vary seeing that only water is removed. Mathematically, it is expressed by:

$$\begin{cases} \frac{dV_f}{dt} = -J \cdot A \\ \frac{dm_{Na_2CO_3}}{dt} = 0 \end{cases}$$

where J is the water flux through the membrane, A its area and t the time. By linearising these equations and by using the relation $m_{Na_2CO_3} = C_{fi} V_{fi}$ (C_f is the Na_2CO_3 concentration), volume $V_{f(i+1)}$ and concentration $C_{f(i+1)}$ at the $(i+1)^{th}$ time step are given by:

$$\begin{cases} V_{f(i+1)} = V_{fi} - J \cdot A \cdot \Delta t \\ C_{f(i+1)} = \frac{C_{fi} \cdot V_{fi}}{V_{f(i+1)}} = \frac{C_{fi} \cdot V_{fi}}{V_{fi} - J \cdot A \cdot \Delta t} \end{cases} \quad (4.13)$$

The quantity of crystals produced is then estimated by the equation:

$$m_{crystals} = (C_{f,end} - C_{f,sat}) V_{f,end} \quad (4.14)$$

Chapter 5

Results and discussions

5.1 Influence of solutions concentration

The results presented in this section follow from the experiments done with the first set-up (see Section 4.2.1) and third set-up (for saturation concentration characterization). Feed and osmotic temperatures were kept at 20°C. Feed and osmotic concentrations varied between the different experiments.

5.1.1 Effects on the flux

Typically, the evolution of the transmembrane flux during the experiments is given in Figure 5.1. Quite logically, the flux decreases with the time. It can be explained on the basis of Equation 2.8. The feed solution loses water but keeps the same amount of Na_2CO_3 . It results from this a feed concentration increase and therefore an activity increase. In the osmotic side, it is the reverse phenomenon. It receives water coming from the feed solution as keeping $NaCl$ mass constant. In consequence, osmotic concentration and activity decrease. Consequently, the activity gradient becomes lower and lower and the flux diminishes. Janssens [2] and Luis et al. [14] also obtained this kind of evolution with experimental time.

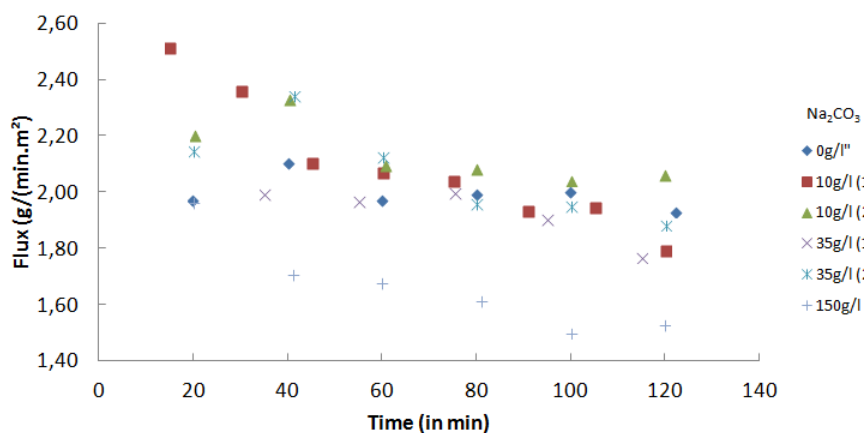


Figure 5.1: Flux evolution during the experiment. $NaCl$ concentration was $300 \frac{g}{l}$. For some Na_2CO_3 concentrations, several experiments were done.

Figure 5.2 shows the dependence of the water flux with respect to the feed concentration. A decreasing relationship is found because a higher feed concentration induces a higher activity and a decrease of the activity gradient, as explained above. Likewise, a lower osmotic concentration brings about a lower flux.

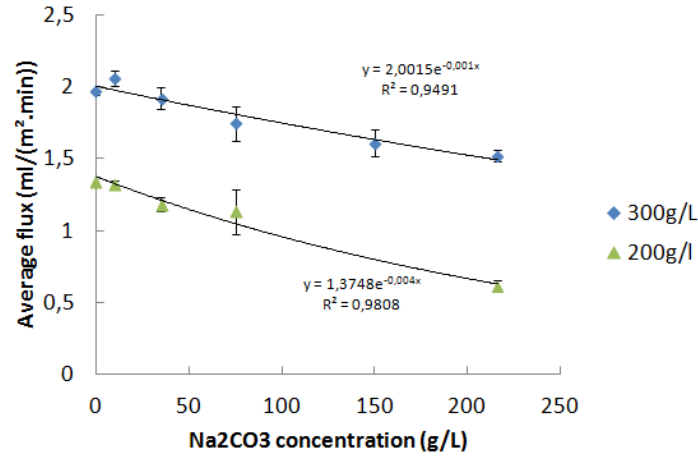


Figure 5.2: Flux evolution in function of the feed concentration, for two $NaCl$ concentrations (200 and 300 $\frac{g}{l}$).

Interpolation curves were drawn on Figure 5.2 in order to be able to predict results in a larger scale. An exponential model was used. It is based on the Equation 4.2 and the exponential dependence of the activity with the concentration, according the used model in Equation A.1. The equation obtained are:

$$J = 2.0015 \exp(-0.001 C_{Na_2CO_3}) \text{ if } C_{NaCl} \approx 300 \frac{g}{l} \quad (5.1)$$

$$J = 1.3748 \exp(-0.004 C_{Na_2CO_3}) \text{ if } C_{NaCl} \approx 200 \frac{g}{l} \quad (5.2)$$

where J is in $\frac{ml}{min.m^2}$ and $C_{Na_2CO_3}$ in $\frac{g}{l}$.

Finally, a last study were done by checking if the assumption according to which concentrations variation during the experiment does not affect the result. Results are available on Figure 5.3. A difference of about $0.17 \frac{ml}{min.m^2}$ is observed, representing approximately 10% of the flux values when concentration is let vary or not.

5.1.2 Effects on mass transfer coefficient

From Figure 5.2, mass transfer coefficients were computed thanks to Equation 4.3. The results were plotted on the Figure 5.4. The first thing that is striking is that the mass transfer coefficient is higher for a $NaCl$ concentration at 200 $\frac{g}{l}$ ($K = 5.87 \pm 0.17 \cdot 10^{-11} \frac{m}{Pa \cdot s}$) than at 300 $\frac{g}{l}$ ($K = 4.72 \pm 0.14 \cdot 10^{-11} \frac{m}{Pa \cdot s}$). It is probably due to a higher polarization phenomena. It could be explained by the fact the higher $NaCl$ concentration withdraws more water from the feed. As a result, the osmotic solution is more diluted near the membrane and the concentration drop between the bulk and the membrane is more accentuated. This phenomenon was also observed by Janssens [2].

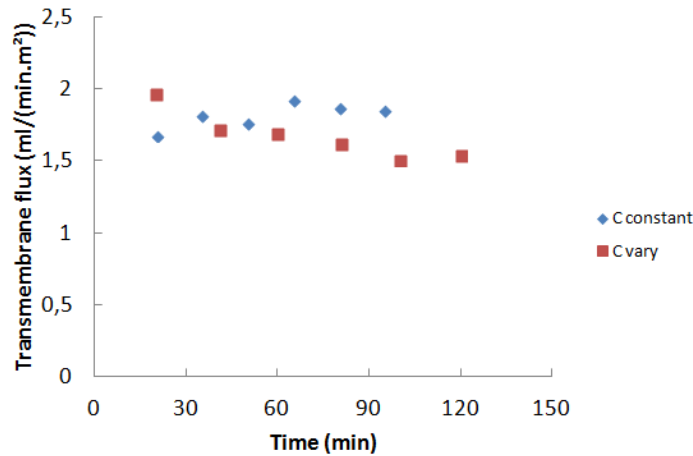


Figure 5.3: Flux evolution in function of time according to whether concentrations are left varying or not. $NaCl$ concentration is $300 \frac{g}{l}$, Na_2CO_3 concentration is $150 \frac{g}{l}$. Average on measures taken on the four last measures of experiments: $1.877 \frac{ml}{min.m^2}$ when concentrations are constant, $1.607 \frac{ml}{min.m^2}$ when they vary.

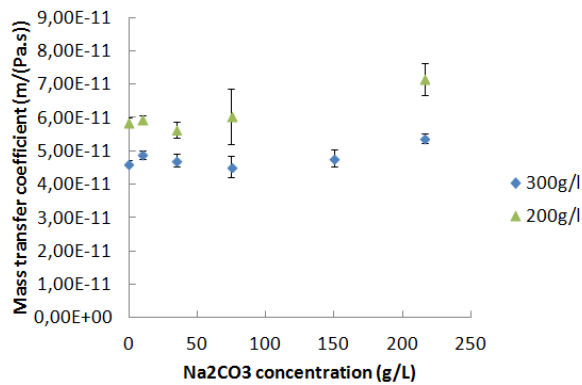


Figure 5.4: Mass transfer coefficient in function of the feed concentration, for two $NaCl$ concentrations (200 and $300 \frac{g}{l}$).

This result is quite interesting to determine the choice of the osmotic concentration in function of the desired objective. The mass transfer coefficient is an indicator of the efficiency of the system. A high mass transfer coefficient means a better utilization of the membrane technology and therefore a better utilization of the energy. If an effective system is wanted, the maximum driving force will be required and the osmotic concentration will be the higher possible (around $300 \frac{g}{l}$). In the opposite, if it is an efficient system that is required, lower osmotic concentration will be used (maybe lower than $200 \frac{g}{l}$). The choice will be determined by an economic optimization by taking into account the quantity produced, the energy cost and the membranes cost.

Another observation that can be done on the basis of the Figure 5.4 is that feed concentration does not affect the mass transfer coefficient. The slight increase for $216 \frac{g}{l}$ is probably due to the fact the measurements were done by another way than the other experiments (see Section 4.3 for further explanations). It could be also related to the fact a higher feed concentration causes a lower driving force and consequently a lower water removal. The difference of concentration between membrane and the bulk is then lower and the concentration polarization too. But notwithstanding this slight

increase at high feed concentration, the flat relationship between the mass transfer coefficient and the feed concentration means that the polarization effect is negligible in the feed side and it is probably the osmotic concentration which is the limiting factor of the mass transfer.

Finally, this study was also done to see if membrane distillation was a possibility to substitute the nanofiltration as concentration step. It results from this study that it could be technically possible. Nevertheless, no information is available about the flux it is possible to obtain with nanofiltration or reverse osmosis. The determination of these fluxes is out of the framework of this thesis and will have to be determined in further research. Moreover, the choice will also be determined by economical criteria. The best condition could also be a combination of the three systems: as it is showed in Figure 2.10 for orange juice for example, one system can be more effective than the others for a certain range of concentration and less for another range. As a conclusion, the optimal combination will result from a trade-off minimising the cost by unit of removed water.

5.2 Influence of temperature

5.2.1 Influence on the transmembrane flux

Dependence of the flux with osmotic temperature has been studied and results are available on Figure 5.5. The first observation is that the flux increases with the osmotic temperature. It is quite surprising as theoretically increasing osmotic temperature decreases the temperature gradient and therefore the partial pressure gradient. By the way, if the inlet temperatures were used to compute the partial pressure gradient when the feed temperature is at 20°C, the flux should be negative. This increase can be explained by the fact that the feed and osmotic temperatures are not the same in the module as in the inlets due to the heat exchange between both sides. For example for osmotic inlet at 25°C and feed inlet at 20°C, it is not 25°C that was measured at the outlet of the osmotic side, but about 20.5°C. And it was 23°C rather than 20°C in the outlet feed. The real temperatures were not the desired ones and they are these temperatures that generate another pressure gradient.

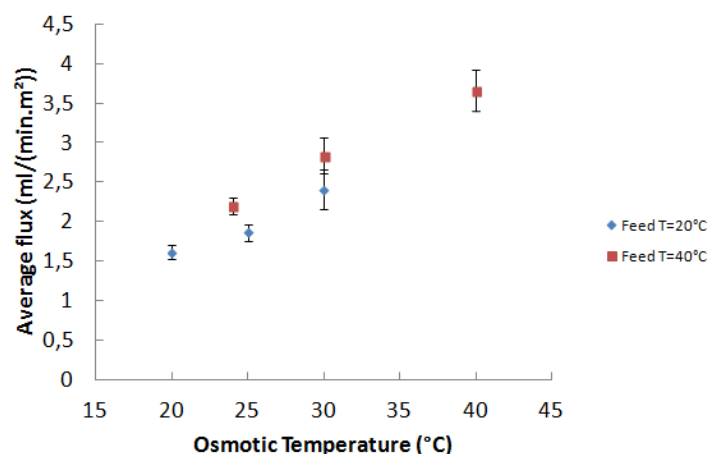


Figure 5.5: Transmembrane flux in function of the osmotic temperature for different feed temperatures. Na_2CO_3 concentration is $150 \frac{g}{l}$ and $NaCl$ concentration is $300 \frac{g}{l}$.

On the contrary, the change of the feed temperature causes the results expected, namely a flux increase in the same time that temperature increase, because of an higher feed partial pressure.

5.2.2 Influence on the mass transfer coefficient

Figure 5.6 shows the mass transfer coefficient calculated from the measured flux. It can be seen the mass transfer coefficient is lower at higher feed temperature. It is bounded to the fact heat is used differently. When the feed temperature is 20°C, the feed is warmed and it gets extra heat from the osmotic to carry out the mass transfer. The performances are higher than the ones expected, which explains the high mass transfer coefficient value. When the feed is at 40°C, it is the contrary: all the heat the feed solution has is not used to carry out the mass transfer. A part of it is lost to warm the osmotic solution or by diffusion through the module. By the way, the difference of mass transfer coefficient between both temperatures at 20° and 40° is mainly due to heat diffusion. Therefore, the performance is lower than the one expected, which explains the lower mass transfer coefficient at 40°C.

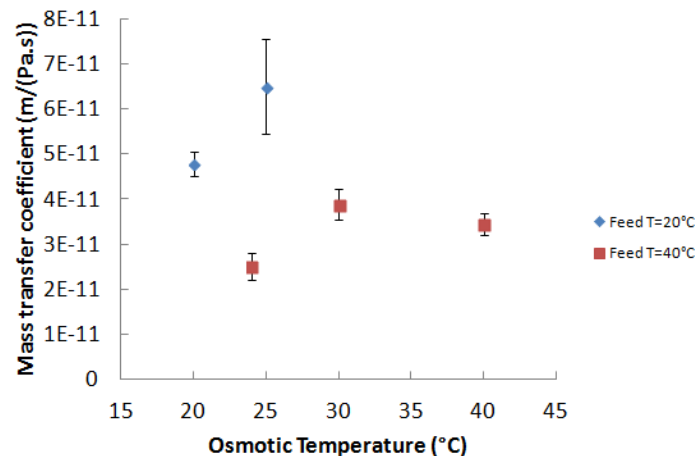


Figure 5.6: Mass transfer coefficient in function of the osmotic temperature for different feed temperatures. Na_2CO_3 concentration is $150 \frac{g}{l}$ and $NaCl$ concentration is $300 \frac{g}{l}$.

In conclusion, in term of quantities exchange, there are advantages to work at higher temperature. But in term of efficiency, it is not always the case as the large part of the energy provided to the system is not used to carry out the mass transfer. Therefore, there is no interest to heat the system by extra combustible burning because it will pollute a lot for a weak gain in effectiveness. It will accuse the environmental interest of the whole process. However, as it is more effective to work at higher temperature and the system is not at very high temperature, residual heat of the process can be used to heat the solutions. The environmental impact will be positively affected in this case because the heat used was basically lost. Therefore the system will be more effective and the heat lost will be lower.

5.3 Crystallization

This section presents the results of the experiments done to study the crystallization, described in Section 4.2.3. Several aspects were studied: the water flux, the duration of the experiments, the crystal purity and the quantity of crystals produced.

5.3.1 Transmembrane flux

Figure 5.7 shows the evolution of the transmembrane flux with the $NaCl$ concentration. As expected, the lower the concentration, the lower the flux. This result highlights the possibility to control

the supersaturation level, which is extremely important in crystallization processes as explained in the Section 2.6.1, by playing with the osmotic concentration. A high concentration of *NaCl* will generate a higher water removal and therefore a higher supersaturation level. On the contrary, low osmotic concentration will induce a lower supersaturation level thanks to a lower water withdrawal.

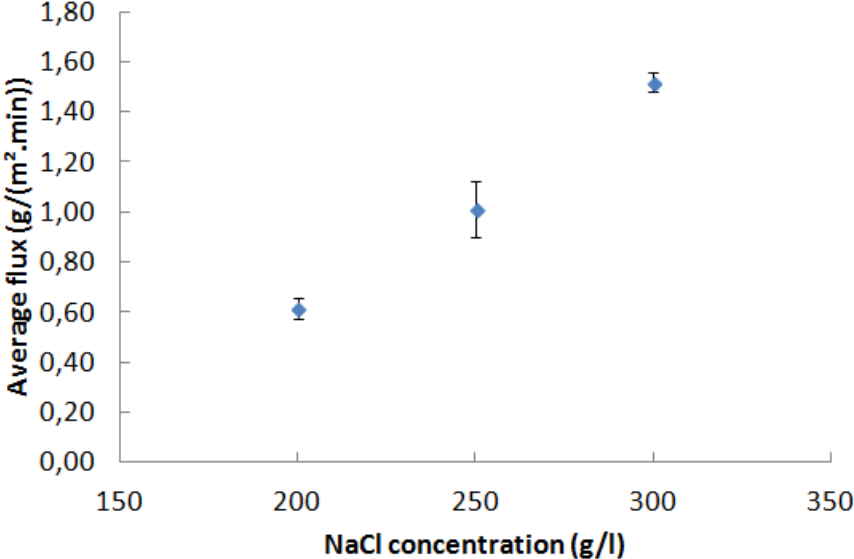


Figure 5.7: Average flux in function of the *NaCl* concentration when *Na₂CO₃* concentration is $215 \frac{g}{l}$.

Figure 5.8 represents the evolution of the mass transfer coefficient in function of the *NaCl* concentration when the feed is in saturation condition. The same conclusion as Section 5.1.2 can be done. A low *NaCl* concentration will lead to a more efficient mass exchange.

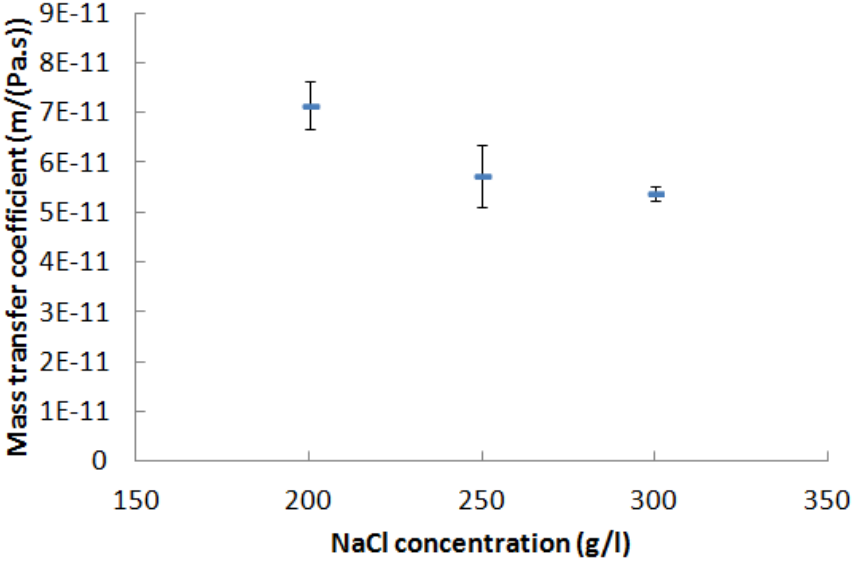


Figure 5.8: Mass transfer coefficient in function of the *NaCl* concentration when *Na₂CO₃* concentration is $215 \frac{g}{l}$.

However, conversely to a concentration step, there are more interests working at lower $NaCl$ concentration in the crystallization step than only being more efficient and spare energy. Indeed the morphology of the crystals will directly depend on the supersaturation level and therefore on the water flux. There are three ways to modify the water flux: modifying the membrane area, modifying the temperature and modifying the osmotic concentration. The first solution is not practical at all in industrial scale: once the process is built, it will not be extended or reduced every day to fulfil the product demands. It would be as if some trays were added to a distillation column to improve the product purity. The second solution could work, but playing with temperature could change the water content of the crystals in addition to require energy. The third solution, changing the osmotic solution, is more advantageous. It requires no energy and all the saturation conditions can be reached if the process is well designed: the membrane area have to be computed to be at the limit of the spontaneous nucleation zone when osmotic flux is maximal ($300 \frac{g}{l}$). The osmotic concentration in the concentration step will not be the same as in the crystallization step, because this one will vary in function of the desired morphology.

5.3.2 Duration before blocking

It is possible to observe on Figure 5.9 the experiment time before blocking appears for different osmotic conditions. As expected, the time needed before reaching blocking increases when the osmotic concentration lowers because the concentration evolution is weaker.

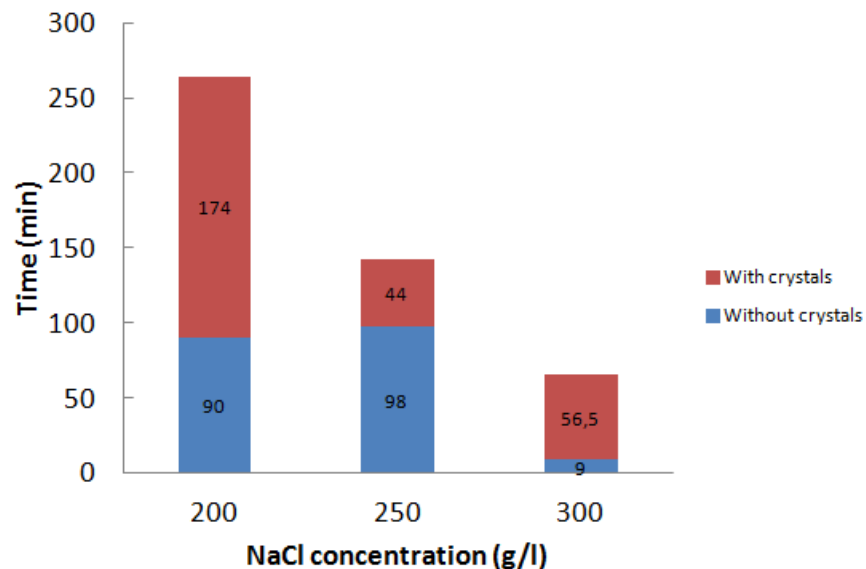
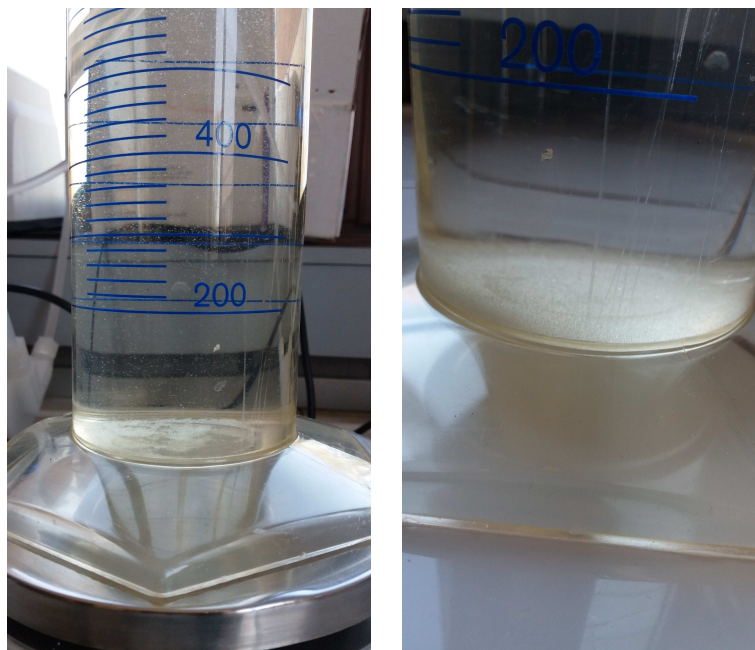


Figure 5.9: Operating duration before blocking appears in function of the osmotic concentration.

However, it could be expected that the time during which crystals are produced and the time passed before first crystals were seen follows the same evolution. Figure 5.9 shows it does not seem to be the case. Actually, reliable conclusion could not be done because a lot of parameters interfere in the smooth running of the experiment. First of all, solubility of Na_2CO_3 is quite temperature dependant and a variation of $0.5^\circ C$ of the initial room temperature can change the solubility of about $6 - 7 \frac{g}{l}$. Therefore, a slight temperature variation between two experiments can increase or decrease by several minutes the time before crystals production. Secondly, the criterion to determine when there are crystals is the eyes of the experimenter which has normally a resolution of some tenths of millimetres. It is

very likely that crystals were present before they were seen and therefore the time of experimentation with crystals should be higher. Finally, the way the experiments were done is problematic. As the solution is constantly recycled, concentration is still increasing until spontaneous nucleation occurs in the membrane and causes its blockage. It will occur sooner than in the continuous conditions wanted for the studied process for which concentration is desired remaining more or less constant.

Technically, the crystals were sensed to be produced in the contactor, grow and then settle in the column. It was not possible to see if crystals were produced in the contactor because fibres diameter is very low ($220\mu m$). In consequence, it is normally the maximum size of the crystals that the membrane can produced. If its size is below $100\mu m$, a normal human eye will not see the crystals leaving the tube. By the way, when crystals were seen leaving the tube, blocking appeared less than 5 minutes later. Afterwards, if crystals grew well in the column, most of them did not settle because the flow was too high and generated too much mixing. As an illustration of the mixing in the column, the flow used were $300\frac{ml}{min}$ and volume of $2l$, residence time was about 6 minutes 40 seconds. As crystals were suspended and not settling (see Figure 5.10a, some of them were absorbed by the feed tube although this one was placed several centimetres above the arrival tube (see Figure 4.4). These crystals, so small they are, were big enough to block the membrane due to the small dimension of the fibres.



(a) Crystals in suspension in the column. (b) Crystals 1 hour after the end of the experiment.

Figure 5.10: Picture of crystals during/after the experiment.

The mixing problem in the feed tank could be solved by two ways. Firstly, residence time could be reduced by using a lower flowrate. An attempt was done by decreasing the flow at $100\frac{ml}{min}$. Unfortunately, it was observed decreasing the flowrate causes much more air in the system, limiting exchanges in the membrane and preventing flow from moving correctly. An alternative could be to change the tank shape and volume. Changing the volume will increase the residence time. Changing the tank shape will allow to favour the settling. Indeed, settling depends on the area of the tank, not its height. A long and wide basin would suit much more as a crystallizer than a column. Unfortunately, no basin without an excessive volume was available. That is why a column was used, by lack of anything better.

As it was explained two paragraphs above, not evolving in perfect continuous conditions leads to a quick blockage of the membrane. That is why experiments attempting to keep concentrations constant were done thanks to the fourth flowsheet (see Section 4.2.4, Table 4.7, first series of experiments). The first experiment ($216\frac{g}{l}$) gives crystals during 30 minutes in the settling column, the whole experiment lasting 47 minutes. The problem occurring during this experiment was the initial concentration was too high, few crystals were present in the feed tank as soon the beginning of the experiment. The other one ($210\frac{g}{l}$) lasted more than 5 hours and crystals were obtained during more than 70 minutes. It would have been able to last longer if experiment was not voluntary stopped. But for this experiment, it was temperature that disturbed the smooth running. Moreover, for both experiments, entrainment problem described before appeared too. For all these reasons, no reliable conclusion could be drawn from these experiments.

To resume, crystallization with membrane was observed possible during at least one hour in clearly non-optimal conditions. It could be expected much more but it needs to be quantify by using another feed tank and paying attention on temperature conditions.

5.3.3 Total water fraction

Total water fraction was characterized for several experiments whose results are identified in Table 5.1. It can be seen that the total water fraction is often between 64% and 66%. Compared to the theoretical values of Table 4.8 in Section 4.4.5, the experimental values are close of 62.94%, corresponding to the decahydrate form ($Na_2CO_3 \cdot 10H_2O$). It could be concluded that it is exclusively the obtained form.

$C_{NaCl} (\frac{g}{l})$	$T_{NaCl} (^{\circ}C)$	$T_{Na_2CO_3} (^{\circ}C)$	TWF (%)
300	20	20	61.25
300	20	20	65.72 ± 1.60
300	20	20	64.29 ± 1.13
300	20	20	64.55 ± 0.22
200	20	20	65.87 ± 1.27
300	25	20	71.58 ± 1.20
300	30	20	65.74 ± 0.54

Table 5.1: TWF for different experimental conditions. Average and standard derivation.

Experiments at higher feed temperature ($34^{\circ}C$ and $40^{\circ}C$ for example) should be interesting to be done regarding Figure 4.8. It should lead to sodium carbonate crystals with lower water content.

5.3.4 Purity

Ten samples were analysed by the Volhard method. A pure water solution, the Na_2CO_3 crystals used to prepare the solution (see Section 4.1.1), $Na_2CO_3 \cdot 10H_2O$ crystals obtained just by dissolving a lot of raw Na_2CO_3 and letting it precipitate and the solution resulting were used as blank. Three crystals samples coming from different experiments and the solutions they were coming from were analysed. Among them, two were done with a fresh Na_2CO_3 , the last one was done with a reused solution.

The test showed there is no Cl^- in sufficient amount to be detected by the method (less than $0.01 \frac{g}{l}$ for the solution, $0.01\%_{wt}$ in crystals). By comparison, Luis et al. [14] obtained with the help of other methods (ion chromatography and x-ray fluorescence) Cl weight percentage of about $1\%_{wt}$, or less, but more than $0.01\%_{wt}$ obtained here. The difference could be explained they used lower osmotic and feed flowrates (between 150 and $350 \frac{ml}{min}$ for osmotic, less than $10 \frac{ml}{min}$ for feed), and they showed that osmotic flowrate influences the Cl content in the crystals. But the contactor they used were smaller and different, which could also explain these results.

It can be concluded from this analyse that Cl transfer from osmotic is very negligible and feed solution and crystals are pure. A long term analysis (on ten or twenty reuses for example) could be interesting to confirm if this tendency carries on with time.

5.3.5 Quantity produced

In order to estimate the quantity of crystals produced, mass evolution was measured about every minute during the entire of the second experiment described in Table 4.6. The water flux related was computed thanks to Equation 4.2. The theoretical concentration evolution was computed thanks to the procedure described in Section 4.4.7. The results are represented in Figure 5.11.

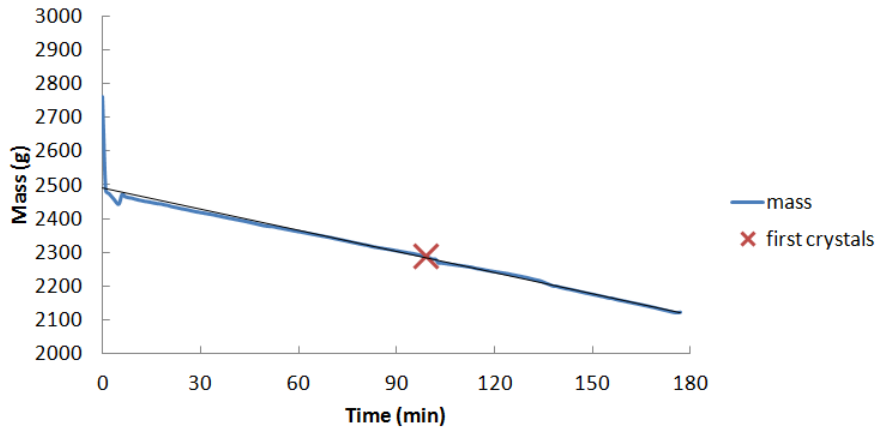
Flux evolution is represented in Figure 5.11b. The numerous peaks are due to the fact the mass were measured each minute and in this short time interval, measurement is sensitive to experimental error. Nevertheless, the results are centred around a mean value, meaning that if measurements were carried out on a much larger time interval (15-20min for example), this effect will be attenuated and much less marked variation observed, at it was the case in all the experiments described above. On Figure 5.11b, it can be seen that two peaks are much more pronounced than the other ones. The first one is the beginning of the experiment, but it is logical because the mass variation is also due to module filling. The other point was just after the observation of the first crystals production. However, both phenomena are not related. The reason of the flux perturbation is big air bubble has formed in the tubes, making the flow circulation by the pump difficult. Then it returns to the normal after the air was hunted.

Produced crystals mass was computed by the Equation 4.14. Final "theoretical" concentration is $241.68 \frac{g}{l}$ and final volume is $1.738l$. The saturation concentration is assumed to be the one corresponding to the first crystals production, being $226.21 \frac{g}{l}$. Therefore, the crystal production is estimated at $26.89g$. It corresponds to 6.40% of the initial Na_2CO_3 mass in the solution.

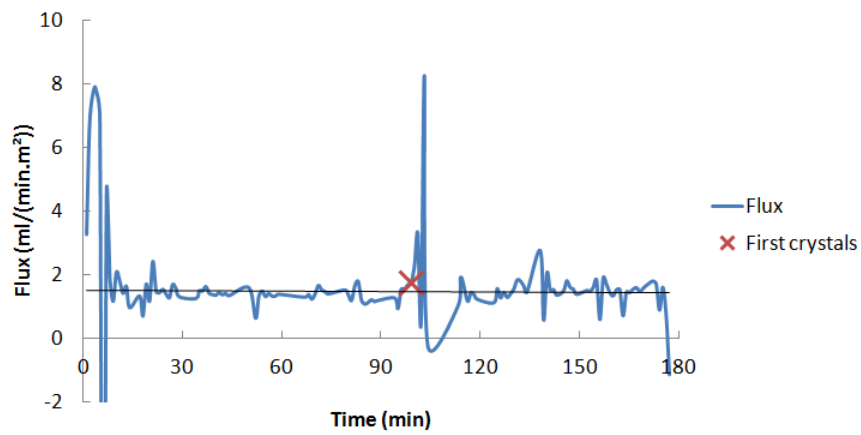
5.4 Influence of the variation of the surface area

5.4.1 Doubling the number of modules

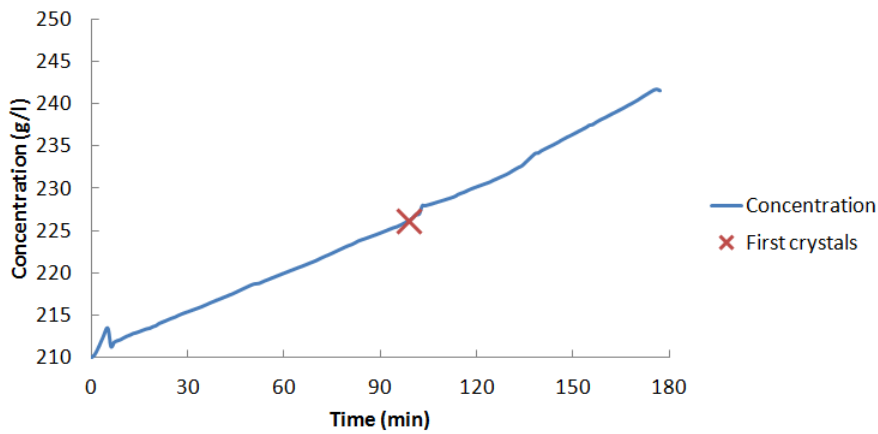
The influence of a slight scale-up on the system was studied thanks to the set-up detailed on Figure 4.6. Figure 5.12 shows how the flux is performing when a extra module is added, increasing the membrane surface from $1.4m^2$ to $2.8m^2$. It can be seen that no significant change appears. Average flux with one module was $1.877 \pm 0.038 \frac{ml}{min.m^2}$ and $1.909 \pm 0.101 \frac{ml}{min.m^2}$ when two modules are used. For the mass transfer coefficient, values are logically close seeing that fluxes are too. $5.589 \pm 0.113.10^{-11} \frac{m}{Pa.s}$ was obtained with one module, $5.684 \pm 0.300.10^{-11} \frac{m}{Pa.s}$ with two modules.



(a) Mass evolution



(b) Flux evolution



(c) theoretical concentration evolution

Figure 5.11: Mass, flux and theoretical concentration evolution during the experiment. Na_2CO_3 initial concentration was $210 \frac{g}{l}$ and $NaCl$ initial concentration was $300 \frac{g}{l}$.

Two further experiments should be done with other concentrations to confirm the result. Afterwards, the system could be scaled up by an order of magnitude (10 – 100 l of solutions, 10 – 100 m² of membrane area) to see if the results are not influenced at a higher scale.

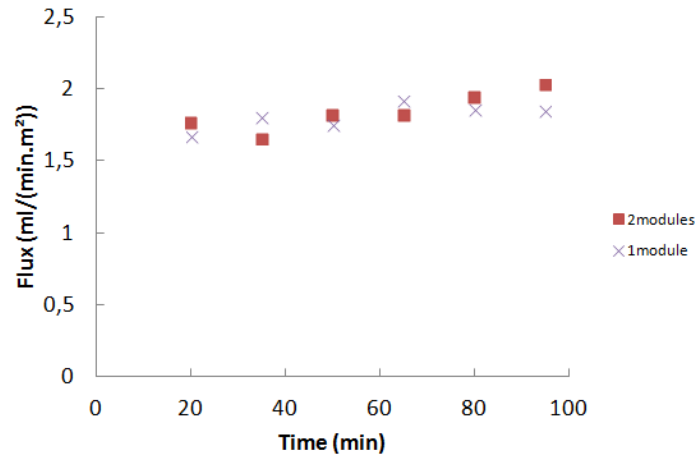


Figure 5.12: Transmembrane flux evolution according the number of modules used. $NaCl$ concentrations are $300 \frac{g}{l}$, Na_2CO_3 concentration is $150 \frac{g}{l}$.

5.4.2 One big or several smaller modules?

The previous result was obtained by adding a module and an osmotic tank to increase the membrane area. Another way to obtain the same result is to increase the module size and using a module of $2.8m^2$ rather than 2 modules of $1.4m^2$. More generally, it can be wondered if it is not more efficient to use a unique big module rather than several smaller modules. A theoretical simulation was done to check this hypothesis.

To compare both cases, it was decided to apply it to the following case. Starting from a feed solution at $150 \frac{g}{l}$, how much membrane surface is it needed to obtain $200 \frac{g}{l}$? Osmotic solutions are supposed to be at $300 \frac{g}{l}$. Feed flowrate is $300 \frac{ml}{min}$, osmotic flowrate is $450 \frac{ml}{min}$ such as the ones used for obtaining the results of Section 5.1. Temperature is $20^\circ C$ too.

One module



Figure 5.13: Schema of one module. Q is the flow, C the concentration. Index f refers to the feed, o to the osmotic, 0 means it is the initial value, f the final one.

Figure 5.13 shows a representation of a single big module to carry out the concentration of the feed. Details of the calculations are available in the Appendix B.1. Q_{ff} , C_{of} and Q_{of} can be computed by a flow and mass balances and are equal to $225 \frac{ml}{min}$, $257.14 \frac{g}{l}$ and $525 \frac{ml}{min}$ respectively. As the concentrations vary a lot in the module and the dependence of flux with concentration is not linear

but rather exponential, the average flux is compute by the way of a logarithmic mean [14]:

$$J_{avg} = K \cdot p^{vap}(T) \frac{(a_{f,in} - a_{p,out}) - (a_{f,out} - a_{p,in})}{\ln(a_{f,in} - a_{p,out}) - \ln(a_{f,out} - a_{p,in})} \quad (5.3)$$

The value of the mass transfer coefficient K is taken at $4.72 \cdot 10^{-11} \frac{m}{Pa \cdot s}$, the value of the coefficient at $150 \frac{g}{l}$ (see Section 5.1.2). The total area needed is obtained by dividing the total water transfer ($75 \frac{ml}{min}$) by the average flux. An area of $59.06 m^2$ is obtained.

Several modules in series

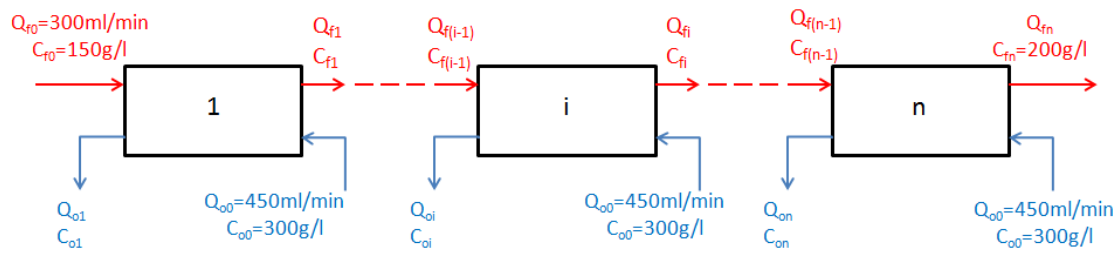


Figure 5.14: Schema of several modules in series. Q is the flow, C the concentration. Index f refers to the feed, o to the osmotic, 0 means it is the initial value and i refers to the values leaving the i^{th} module.

A schema of the system is represented on the Figure 5.14. The details of the calculations are available in Appendix B.2. Each module has a surface membrane of $1.4 m^2$. Here, balances are just done on each step. The flux in each module changes because it is not the same concentration at their inlet. The flux in each module is given by Equation 5.1. As flow and concentration are known before the first module, the one at the inlet of the second one can be computed, then the one at the inlet of the third one and so on by iteration until the $200 \frac{g}{l}$ are reached. Results are it needs to use 32 modules in series to reach the desired concentration, either $44.80 m^2$.

Explanation

The reason of this difference is quite simple to understand. By using several modules, it is possible to use several osmotic supplies. Therefore, the osmotic flow is "refreshed" steadily along the concentration path, allowing to keep an osmotic concentration as high as possible and therefore a high flux. This is not possible when only one module is used. The osmotic concentration decreases steadily and at the end, the transmembrane flux is low. Therefore, to have the same results, membrane area have to be increased or higher osmotic flowrate have to be used. Using only one big module will very often be worse than using several ones.

5.5 Practical example

As an illustration, results obtained in the previous sections will be used to size a possible practical case. The different steps will be a membrane absorption with $NaOH$, a membrane distillation as concentration step and finally the membrane crystallization.

CO₂ production by the power plant

The case studied was to treat the CO₂ emissions of a 330MW power plant, fed with 98.16 $\frac{kg}{s}$ of coal with a carbon content of 22.58%_{wt} [22]. The input of carbon is therefore 22.17 $\frac{kg}{s}$. If assumption is made that all this carbon is converted in CO₂, the number of moles of CO₂ is the same of the number of moles of carbons. Therefore, there are 1848 $\frac{mol}{s}$ of CO₂ produced, being 81.312 $\frac{kg}{s}$ or 149150Nm³/h.

Membrane absorption

This step was not studied in the framework of the project. That is why no membrane area calculation needed for membrane absorption will be done. However, it could be interesting to have an idea of the Na₂CO₃ concentration it could be expected at the end of this step.

According to Yoo et al [20], NaOH has a very good affinity with CO₂. A yield of nearly 100% can be assumed if sufficient quantity of NaOH is used. That is why a NaOH stream of 1M is used. On one hand to have a large quantity of NaOH to capture CO₂. On the other hand, such a concentration allows to have a high pH (about 14) and prevent HCO₃⁻ formation.

As two moles of NaOH is needed to capture one mole of CO₂, 3696 $\frac{mol}{s}$ of NaOH is needed to capture the CO₂ from the power plant and produce 1848 $\frac{mol}{s}$ of Na₂CO₃. As the concentration of NaOH is 1M, the solution flow is 3696 $\frac{l}{s}$. The Na₂CO₃ concentration at the outlet of the membrane absorption is therefore 0.5 $\frac{mol}{l}$ or 53 $\frac{g}{l}$.

Membrane distillation

This step consists in a following of modules of 1.4m² to be able to use the results obtained experimentally. The NaCl concentration is 300 $\frac{g}{l}$. Temperature is of about 20°C. The objective is to reach a Na₂CO₃ concentration of 216 $\frac{g}{l}$, the saturation concentration. The same methodology of calculation as the several modules in series case described in Section 5.4.2 were used (see Appendix B.2 for details). A surface of 9.236 · 10⁷ m² and a volume of 36285m³ (volume of a module: about 0.55l) will be required. The flow is about 906.9 $\frac{l}{s}$.

Membrane crystallization

The principle of calculation is the same of membrane distillation. The difference is the concentration aimed will depend of the quality of crystals wanted. Moreover, the initial concentration is 216 $\frac{g}{l}$. Table 5.2 holds the quantity of crystals produced and the surface area needed to obtain this result with a 300 $\frac{g}{l}$ NaCl osmotic flow.

In total, the membrane area required for membrane distillation and membrane crystallization is quite important (9 – 10 · 10⁷ m²) which means high investment costs. In term of space needed, it represents about 36000m³. It means that a cubic space of 33m dimension can hold all the membrane area. Nevertheless, results computed above have to be taken with care. Modules used for calculation are the ones of the lab (1.4m² in a volume of 0.55l) whereas industrial modules provided by Liqui-Cel® can have volumes of about 80l containing 373m² of membranes [43].

Na_2CO_3 ($\frac{g}{l}$)	membrane area (m^2)	Total volume (m^3)	flow ($\frac{l}{s}$)	$m_{crystals}$ ($\frac{kg}{h}$)
217	155600	61.13	902.7	3250
218	309900	121.74	898.6	6470
219	462900	181.85	894.4	9660
220	614700	241.49	890.4	12822

Table 5.2: Membrane area required for the crystallization step of a capture system for 330MW power plant, as well the quantity of crystals produced.

Chapter 6

Conclusion

Developing efficient systems allowing to capture CO_2 is a primordial concern of today in the struggle against greenhouse gases emissions. Membrane technologies contain several advantages such as low energy consumption and better mass exchange to fulfil this function. That is why membrane absorption, nanofiltration, membrane distillation and membrane crystallization are used in such a system that is under research in which this thesis places itself.

It emerges from this work that the last step is technically possible. Crystals can be obtained in a durable way in condition suitable tanks with high enough volume are used to avoid entrainment of the crystals in the membrane. Crystals forms at $20^\circ C$ are in the form $Na_2CO_3 \cdot 10H_2O$. The membrane allows perfectly to separate the Na_2CO_3 solution from the $NaCl$ one used to generate the water removal, so that no chloride were found in the crystals formed.

$NaCl$ concentration will influence the water flux because it impacts the activity gradient. With $300 \frac{g}{l}$, the water flux will vary between $2.10 \frac{ml}{min \cdot m^2}$ and $1.50 \frac{ml}{min \cdot m^2}$ when the Na_2CO_3 concentration decreases. When $NaCl$ concentration is $200 \frac{g}{l}$, the flux varies between $1.35 \frac{ml}{min \cdot m^2}$ and $0.60 \frac{ml}{min \cdot m^2}$. However, the membrane performances are better used with a lowest $NaCl$ concentration due to the decrease of concentration polarization, which is translated by a higher mass transfer coefficient ($5.87 \frac{m}{Pa \cdot s}$ for $200 \frac{g}{l}$, $4.72 \frac{m}{Pa \cdot s}$ for $300 \frac{g}{l}$).

Membrane distillation can also be carried out by a temperature difference. The higher the temperature in each side will be, the higher the flux will be. However, a better energy utilization will be realised if the $NaCl$ temperature is higher than the Na_2CO_3 one.

Finally, a big practical advantage of membrane system is the linear scale-up possibility. Adding another membrane module doubles the water flux. However, experiments have to be carried out with more modules to see if the tendency will go on.

If results are quite promising for an industrial use, further research and improvements remains to be done. Crystallization have to be studied with more appropriated tanks (higher volume and more optimized shape) to let crystals settle and grow. Afterwards, it has to be studied at higher temperature ($40 - 50^\circ C$) to form crystals with lower water content ($Na_2CO_3 \cdot H_2O$). Moreover, this thesis only focused on membrane distillation-crystallization which is only one step of the overall process. More research on membrane absorption and nanofiltration have to be done in order to know if this process could be implemented in industry and really limit CO_2 emissions without being a big economic obstacle.

Bibliography

- [1] M. McGee, "Co2.earth." <http://www.co2.earth/>. visited the 8th of December 2015.
- [2] R. Janssens, "Co2 valorization as na2co3 crystals by using membrane distillation crystallization," Master's thesis, Université catholique de Louvain, 2015.
- [3] World Meteorological Organization, "The state of greenhouse gases in the atmosphere based on global observations through 2014," *Greenhouse Gas Bulletin*, vol. 11, 2015.
- [4] I. Ruiz Salmon, "Phd project," September 2014.
- [5] EIPPCB and TWG, "Integrated pollution prevention and control reference document on best available techniques for large combustion plants," in *Integrated Pollution Prevention and Control*, pp. 1–618, European Commission, July 2006.
- [6] M. Songolzadeh, M. Soleimani, M. T. Ravanchi, and R. Songolzadeh, "Carbon dioxide separation from flue gases: A technological review emphasizing reduction in greenhouse gas emissions," *The Scientific World Journal*, vol. 2014, 2014.
- [7] H. Susanto, "Towards practical implementations of membrane distillation," *Chemical Engineering and Processing: Process Intensification*, vol. 550, pp. 139–150, 2011.
- [8] J. G. J. Olivier, G. Janssens-Maenhout, M. Muntean, and J. A. H. W. Peters, "Trends in global co2 emissions; 2013 report.," tech. rep., The Hague: PBL Netherlands Environmental Assessment Agency; Ispra: Joint Research Center, 2013.
- [9] M. Wang, A. S. Joel, C. Ramshaw, D. Eimer, and N. M. Musa, "Process intensification for post-combustion co2 capture with chemical absorption: A critical review," *Applied Energy*, vol. 158, pp. 275–291, 2015.
- [10] P. Luis, T. Van Gerven, and B. Van der Bruggen, "Recent developments in membrane-based technologies for co2 capture," *Progress in Energy and Combustion Science*, vol. 38, pp. 419–448, 2012.
- [11] P. Luis and B. Van der Bruggen, "The role of membranes in post-combustion co2 capture," *Greenhouse Gas Science and Technology*, vol. 3, pp. 1–20, 2013.
- [12] W. Ye, J. Lin, J. Shen, P. Luis, and B. Van der Bruggen, "Membrane crystallization of sodium carbonate for carbon dioxide recovery: Effect of impurities on the crystal morphology," *Crystal Growth and Design*, vol. 13, pp. 2363–2372, 2013.
- [13] P. Luis, B. Van der Bruggen, and T. Van Gerven, "Non-dispersive absorption for co2 capture: from the laboratory to industry," *Journal of Chemical Technology and Biotechnology*, vol. 86, pp. 769–775, 2011.
- [14] P. Luis, D. Van Aibel, and B. Van der Bruggen, "Technical viability and exergy analysis of membrane crystallization: Closing the loop of co2 sequestration," *Internationnal Journal of Greenhous Gas Control*, vol. 12, pp. 450–459, 2013.

- [15] D. Jansen, M. Gazzania, G. Manzolini, E. van Dijk, and M. Carbo, "Pre-combustion co₂ capture," *International Journal of Greenhouse Gas Control*, vol. 40, pp. 167–187, 2015.
- [16] E. S. Rubin, H. Mantripragada, A. Marks, P. Versteeg, and J. Kitchin, "The outlook for improved carbon capture technology," *Progress in Energy and Combustion Science*, vol. 38, pp. 630–671, 2012.
- [17] M. Aneke and M. Wang, "Process analysis of pressurized oxy-coal power cycle for carbon capture application integrated with liquid air power generation and binary cycle engines," *Applied Energy*, vol. 154, pp. 556–566, 2015.
- [18] W. Li, B. Van der Bruggen, and P. Luis, "Recovery of na₂co₃ and na₂so₄ from mixed solutions by membrane crystallization," *Chemical Engineering Research and Design*, vol. 106, pp. 315–326, 2016.
- [19] P. Keshavarz, J. Fathikalajahi, and S. Ayatollahi, "Analysis of co₂ separation and simulation of a partially wetted hollow fiber membrane contactor," *Journal of Hazardous Materials*, vol. 152, pp. 1237–1247, 2008.
- [20] M. Yoo, S.-J. Han, and J.-H. Wee, "Carbon dioxide capture capacity of sodium hydroxide aqueous solution," *Journal of Environmental Management*, vol. 114, pp. 512–519, 2013.
- [21] P. Luis, "Use of monoethanolamine (mea) for co₂ capture in a global scenario: Consequences and alternatives," *Desalination*, vol. 380, pp. 93–99, 2016.
- [22] I. Vorrias, K. Atsonios, A. Nikolopoulos, N. Nikolopoulos, P. Grammelis, and E. Kakaras, "Calcium looping for co₂ capture from a lignite fired power plant," *Fuel*, vol. 113, pp. 826–836, 2013.
- [23] A. A. Merdaw, A. O. Sharif, and G. A. W. Derwish, "Mass transfer in pressure-driven membrane separation processes, part ii," *Chemical Engineering Journal*, vol. 168, pp. 229–240, 2011.
- [24] J. D. Seader, E. J. Henley, and D. K. Roper, *Separation process principles: Chemical and Biochemical Operations*. John Wiley & Sons, 3rd ed., 2011.
- [25] T. Leyssens and P. Adam, "Solid-fluid separation." Université Catholique de Louvain, 2015. Course taught in Université Catholique de Louvain.
- [26] W. Zhang, J. Luo, L. Ding, and M. Y. Jaffrin, "A review on flux decline control strategies in pressure-driven membrane processes," *Industrial & Engineering Chemistry Research*, vol. 54, p. 2843–2861, 2015.
- [27] R. Lakerveld, J. Kuhn, H. J. M. Kramer, P. J. Jansens, and J. Grievink, "Membrane assisted crystallization using reverse osmosis: Influence of solubility characteristics on experimental application and energy saving potential," *Chemical Engineering Science*, vol. 65, pp. 2689–2699, 2010.
- [28] A. A. Merdaw, A. O. Sharif, and G. A. W. Derwish, "Mass transfer in pressure-driven membrane separation processes, part i," *Chemical Engineering Journal*, vol. 168, pp. 215–228, 2011.
- [29] E. Drioli, A. Criscuoli, and E. Curcio, *Membrane contactors: Fundamentals, applications and potentialities*, vol. 11 of *Membrane Science and Technology*. Elsevier, 2006.
- [30] G. Chen, Y. Lu, W. B. Krantz, R. Wang, and A. G. Fane, "Optimization of operating conditions for a continuous membrane distillation crystallization process with zero salty water discharge," *Journal of Membrane Science*, vol. 450, pp. 1–11, 2014.
- [31] W. Li, B. Van Der Bruggen, and P. Luis, "Integration of reverse osmosis and membrane crystallization for sodium sulphate recovery," *Chemical Engineering and Processing: Process Intensification*, vol. 85, pp. 57–68, 2014.

- [32] M. Brito Martínez, N. Jullok, Z. Rodríguez Negrín, B. Van der Bruggen, and P. Luis, “Membrane crystallization for the recovery of a pharmaceutical compound from waste streams,” *Chemical Engineering Research and Design*, vol. 92, pp. 264–272, 2014.
- [33] W. Ye, J. Lin, H. T. Madsen, E. G. Søgaard, C. Hélix-Nielsen, P. Luis, and B. Van der Bruggen, “Enhanced performance of a biomimetic membrane for Na_2CO_3 crystallization in the scenario of CO_2 capture,” *Journal of Membrane Science*, vol. 498, pp. 75–85, 2016.
- [34] Liqui-Cell®membrane contactor, “2.5x8 extra-flow data sheet,” 2015. consulted the 14th May 2016.
- [35] E. Chabanon, D. Mangin, and C. Charcosset, “Membranes and crystallization processes: State of the art and prospects,” *Journal of Membrane Science*, vol. 509, pp. 57–67, 2016.
- [36] X. Jiang, D. Lu, W. Xiao, X. Ruan, J. Fang, and G. He, “Membrane assisted cooling crystallization: Process model, nucleation, metastable zone, and crystal size distribution,” *American Institute of Chemical Engineers Journal*, vol. 62, pp. 829–841, March 2016.
- [37] E. Curcio and E. Drioli, “Membrane distillation and related operations — a review,” *Separation and Purification Reviews*, vol. 34, pp. 35–86, 2005.
- [38] G. Zuo, R. Wang, R. Field, and A. G. Fane, “Energy efficiency evaluation and economic analyses of direct contact membrane distillation system using aspen plus,” *Desalination*, vol. 283, pp. 237–244, 2011.
- [39] D. Singh and K. K. Sirkar, “Desalination of brine and produced water by direct contact membrane distillation at high temperatures and pressures,” *Journal of Membrane Science*, vol. 389, pp. 380–388, 2012.
- [40] D. Singh and K. K. Sirkar, “High temperature direct contact membrane distillation based desalination using ptfе hollow fibers,” *Chemical Engineering Science*, vol. 116, pp. 824–833, 2014.
- [41] E. Drioli, G. Di Profio, and E. Curcio, “Progress in membrane crystallization,” *Current opinion in Chemical Engineering*, vol. 1, pp. 178–182, 2012.
- [42] College of Science, University of Canterbury, “Determination of chloride ion concentration by titration (volhard’s method).” http://www.outreach.canterbury.ac.nz/chemistry/documents/chloride_volhard.pdf.
- [43] Liqui-Cell®membrane contactor, “14x40 extra-flow product data sheet.” http://www.liquicel.com/uploads/documents/14x40-D102Rev4-10-15%20_ke2.pdf, 2015. consulted the 4th June 2016.
- [44] S. I. Sandler, *Chemical, biochemical and engineering thermodynamics*. John Wiley & Sons, 6th ed., 2006.
- [45] D. W. Green and R. H. Perry, *Perry’s chemical engineer’s handbook*. McGraw Hill, 8th ed., 2008.

